Article:
Zou, J, Ziegler, AD, Chen, D et al. (2022) Rewetting global wetlands effectively reduces major greenhouse gas emissions. Nature Geoscience, 15 (8). pp. 627-632. ISSN: 1752-0894

https://doi.org/10.1038/s41561-022-00989-0

Rewetting global wetlands effectively reduces major greenhouse gas emissions

Junyu Zou[1], Alan D. Ziegler[2], Deliang Chen[3], Gavin McNicol[4], Philippe Ciais[5], Xin Jiang[1], Chunmiao Zheng[1], Jie Wu[1,6], Jin Wu[7,8], Ziyu Lin[1,7], Xinyue He[1,9], Lee E. Brown[10], Joseph Holden[10], Zuotai Zhang[1], Sorain J. Ramchunder[11], Anping Chen[12], Zhenzhong Zeng[1*]

[1] School of Environmental Science and Engineering, Southern University of Science and Technology, Shenzhen 518055, China

[2] Faculty of Fisheries and Aquatic Resources, Mae Jo University, Chiang Mai, Thailand

[3] Regional Climate Group, Department of Earth Sciences, University of Gothenburg, Gothenburg, Sweden

[4] Department of Earth and Environmental Science, University of Illinois, Chicago, Chicago, Illinois, United States

[5] Laboratoire des Sciences du Climat et de l'Environnement (LSCE), CEA CNRS UVSQ, 91191 Gif Sur Yvette, France

[6] Department of Geoscience and Natural Resource Management, University of Copenhagen, Copenhagen, Denmark

[7] School of Biological Sciences and Institute for Climate and Carbon Neutrality, The University of Hong Kong, Pokfulam Road, Hong Kong, China

[8] State Key Laboratory of Agrobiotechnology, The Chinese University of Hong Kong, Hong Kong, China

[9] School of Earth and Environment, University of Leeds, Leeds, UK

[10] water@leeds, School of Geography, University of Leeds, Leeds, UK

[11] Department of Geography, National University of Singapore, Singapore, Singapore

[12] Department of Biology and Graduate Degree Program in Ecology, Colorado State University, CO 80523, USA

* Correspondence to: zengzz@sustech.edu.cn

Manuscript for *Nature Geoscience*

May 9, 2022

Carbon and nitrogen losses from degraded wetlands, and methane emissions from flooded wetlands, are both significant sources of greenhouse gas emissions. However, the net exchange dependence on hydro-thermal conditions and wetland integrity remains unclear. Using a global-scale *in-situ* database on net greenhouse gas exchanges, we show diverse hydrology-influenced emission patterns in CO_2, CH_4 and N_2O. We find that total CO_2 equivalent emissions from wetlands are kept to a minimum when the water table is near the surface. In contrast, greenhouse gas exchange rates peak in flooded and drained conditions. By extrapolating the current trajectory of degradation, we estimate that between 2021 and 2100, wetlands could result in greenhouse gas emissions equivalent to around 408 gigatons of CO_2. However, rewetting wetlands could reduce these emissions such that the radiative forcing caused by CH_4 and N_2O is fully compensated by CO_2 uptake. As wetland greenhouse gas budgets are highly sensitive to changes in wetland area, the resulting impact on climate from wetlands will depend on the balance between future degradation and restoration.

Wetlands have continuously accumulated organic carbon since the Last Glacial Maximum[1], forming a dense carbon pool that stores over one third of global soil organic carbon in only 6% of the total land area[2,3]. Alarmingly, since the Industrial Revolution, more than half of wetlands have been degraded by anthropogenic activities, including drainage, deforestation, afforestation, agricultural expansion, urbanization, and climate change[4-8]. A phenomenon commonly associated with wetland degradation is the lowering of the water table, which exposes carbon pools above the water table to decomposition and releases CO_2, while simultaneously altering the natural exchange of other greenhouse gases (GHGs) including methane (CH_4) and nitrous oxide (N_2O)[9-11]. Given that degraded wetlands are important sources of GHG emissions to the atmosphere[11-14], there is a

critical need to determine the impact of widespread wetland degradation on GHG exchanges, but also to assess the potential for wetland restoration in reducing GHG emissions.

Fluxes of CO_2, CH_4, and N_2O in wetlands are mediated by the water level relative to the surface[9,15-16]. Electron acceptor limitation in the soils of saturated wetlands is favorable to the production of methane[17,18], forming the world's largest natural source of CH_4 emissions[12]. Meanwhile, substantial CO_2 is consumed through photosynthesis by wetland vegetation; and the anaerobic conditions significantly reduce the decomposition of organic carbon, generating a major terrestrial carbon sink over long time scales[1-3,19,20]. By contrast, the degradation of wetlands, either through drainage or desiccation, exposes stored organic matter to aerobic decomposition, resulting in the emission of CO_2 and N_2O to the atmosphere[11,15,16,21]. Previously, the relationship between GHG emissions and water table in wetlands has been examined for only one or two greenhouse gases[22], and for one single wetland category (e.g. managed peatland[14,23,24]) or various wetland categories at local scales[11,25,26]. Lacking is a global assessment involving the three main GHGs to guide the development of effective climate change mitigation strategies and to inform the potential to restore the functioning of wetland ecosystems across moisture and temperature regimes worldwide.

We address this issue by building a global database containing *in-situ* observations of exchange rates of GHGs for wetlands, drawn from 3,704 site-year records (Extended Data Figure 1; refer to *Methods* for details). Each record contains data on wetland environmental conditions and flux information that allows quantitative assessments of the net fluxes of CO_2, CH_4, and N_2O under various wetness conditions. The reported details of the environmental conditions from each site-year record allow us to perform a novel multi-gas assessment for a variety of wetland types and

moisture regimes worldwide. In doing so we classify the wetness condition of each site-year in the growing season into six categories that are related to the water-table/level (*WTL*) depth below (negative number) and above (positive) the surface: *WTL*-3 ≤ -70 cm; -70 cm < *WTL*-2 ≤ -50 cm; -50cm < *WTL*-1 ≤ -30 cm; -30 cm < *WTL0* ≤ -5 cm; -5 cm < *WTL*1 ≤ 40cm; and 40 cm < *WTL*2. We illustrate differences related to temperature regimes by assessing responses across three climate zones (boreal, temperate, and tropical; defined by thresholds of multi-year average surface air temperature).

The non-linear hydro-thermal influence on GHG exchange

We call the CO_2 net-exchange flux at the water/land-atmosphere interface net ecosystem exchange (*NEE*) (Equation 1; positive/negative values indicate GHG sources/sinks). Through establishing relationships between *NEE* and the total GHG flux (sum of CO_2, CH_4, and N_2O in CO_2 equivalent) based on the records containing complete data, we observe the following: (1) almost all (173/174) records show the total GHG flux values exceed *NEE* for the same site-year, and (2) the differences between the NEE and total GHG flux are highly dependent on moisture conditions (Figures 1a-b). These results indicate clearly that the wetness regulation pattern for CH_4 or N_2O emissions is different from CO_2 (ref. 27). By mapping the distribution of wetness control for the three GHGs for various types of wetlands (inter alia bogs, fens, marshes, swamps, floodplain and water bodies; see *Methods*), we identify nonlinear (parabolic) exchange patterns for *NEE* and the sum of GHGs, and opposing monotonic patterns for CH_4 and N_2O (Figures 1c-f, Extended Data Figures 2a-b, 3b, 4a-b). Maximum emission of CH_4 occurs when flooded wetlands have water levels well above the soil surface (*WTL2*; water level > 40 cm); and the minimum occurs when the water table is well below the surface of the wetland (*WTL*-2&-3; water table ≤ -50 cm), indicative of a drained or

desiccated state. In contrast, the highest emissions of N_2O occur during dry conditions (*WTL*-3); and the lowest occur in flooded conditions (*WTL*2). Emissions of CO_2 exhibit relative extremes both for high water level and low water-table conditions (Figure 1d, Extended Data Figure 4b).

These hydrology-dependent emission patterns are in line with the expectation that CH_4 is produced in the anaerobic conditions that are associated with waterlogged soils[21,28]. Lower emissions of N_2O occur during flooded conditions because facultative anaerobic denitrifying bacteria reduce N_2O to N_2 in the oxygen-depleted water column[21,29]. As the water table falls below the soil surface, aerobic decomposition of organic matter results in an increase in CO_2 emissions[11,15,21]. As expected, the highest CO_2 emission was observed in *WTL*-3, where the water table is lower than 70 cm (Figure 1d, Extended Data Figure 4a). The relatively high CO_2 emissions observed in wetlands under flood conditions (*WTL*2) are likely driven by the lateral movement of organic matter across the landscape, the leaching of organic carbon into a dissolved state, and subsequent oxidation by heterotrophs[30,31]. Finally, the lowest emission of the sum of all three GHGs (CO_2, CH_4, and N_2O) occurs when the water table is near the ground surface (*WTL0*; ranging from -30 cm to -5 cm), with near zero emissions. This nonlinear wetness pattern is in agreement with the recent report by Evans *et al.*[24] which only studied selected peatland sites and did not incorporate N_2O (Extended Data Figure 2a-b).

The parabolic pattern in GHG flux varies across boreal, temperate, and tropical regimes (Figure 2, Extended Data Figure 3b), demonstrating that climate influences the dependency of wetland GHG emission on the wetness regime. The net GHG flux in each temperature regime tends to be approximately neutral when the water table is near the ground surface, although it requires higher

WTL (-5~40 cm) to approach GHG equilibrium for the tropical sites (see Figure 2c, Extended Data Table 1). Using the empirical GHG exchange rates in the *WTL*2 group for different temperature regimes (*Methods*), we estimate the annual GHG emissions from global water bodies (lakes & reservoirs) to be 1.0 Gt yr^{-1} CO_2 and 127.5 Tg yr^{-1} CH_4, which are similar to the previous reports[32,33] of 1.2 Gt yr^{-1} CO_2 and 175.2 Tg yr^{-1} CH_4 (Supplementary Figure S1). In addition, we estimate the CH_4 emission from natural freshwater wetlands to be 144.4 Tg per year, corresponding well with the 148.6 Tg CH_4 reported by ref. 12. Furthermore, the GHG emissions per area for wetlands with a low water table (*WTL* ≤ -70 cm) are 19.7 and 11.2 tCO_2eq ha^{-1} yr^{-1} for boreal and temperate regimes, respectively. These values are consistent with both Evans *et al.* [24] (17.60 t CO_2eq ha^{-1} yr^{-1} in the case of -70cm water level) and Leifeld *et al.*[13] who determined the drainage-related GHG emission rates for boreal & temperate zones (16.1 tCO_2eq ha^{-1} yr^{-1}). These validated empirical values in the nonlinear relationship between *WTL* and GHG emissions then represent a novel opportunity to assess the global GHG emissions resulting from wetland degradation.

GHG emissions from wetland degradation

We evaluate past and future scenarios of wetland degradation by integrating the natural Wetland Extent Trends (WET) index[4,5] (Supplementary Figure S2) with the Global Lakes and Wetlands Database[34] (GLWD). We assess the historical emissions from degraded wetlands at the global scale based on GHG intensities at low (deep) water table conditions, which reflect wetland drainage/desiccation (*WTL*-3 ≤ -70 cm; Extended Data Table 1, Supplementary Figure S3). Historically, over the past 71 years (1950 to 2020), 46.22% of global wetlands have been degraded (4.85 Mkm^2), producing 276.4±175.5 Gt CO_2eq (95% confidence interval of GHG emissions) to

the atmosphere (Figure 3a, Extended Data Table 2). Russia, Brazil, and Canada were the largest emitters because of their vast wetland areas with a high density of soil organic carbon, contributing to nearly one half of global wetland GHG emissions: 18.6%, 15.1%, and 14.6%, respectively (Figures 3b, 4a, Extended Data Figure 5a).

Following a history-derived, business-as-usual scenario for the future, we project that continued wetland degradation (7.76 Mkm^2, 74.0%) would release an estimated total of 407.9±251.5 Gt CO_2eq into the atmosphere from 2021 to the end of the 21st century (Figure 4b). Of these, 155.6 Gt CO_2eq (38.1%) were emitted from freshwater marsh and floodplain, and 96.7 Gt CO_2eq (23.7%) from peatlands, with the latter emitting an average of 1.21 Gt per year, which is consistent with 1.32 Gt yr^{-1} or 1 Gt yr^{-1} reported by Günther *et al.*[14] and Ojanen *et al.*[23]. Carbon dioxide would contribute the highest emissions: 306.1±159.4 Gt (Extended Data Figure 6; Extended Data Table 2). Regionally, 71.1%, 4.6%, and 24.3% of the GHG emissions would be from boreal, temperate, and tropical regions, respectively. The estimate for the tropics is lower than that reported by Leifeld *et al.*[13], because we consider the depletion of the carbon pool during 2021-2100 (Extended Data Figure 7). Furthermore, we recognize the potential for strong, positive climate feedback in the boreal region stemming from the loss of substantial carbon storage in the future[11,35].

Emission reduction potential under rewetting scenarios

To explore the potential for reducing GHG release from degraded wetlands, we consider two peak clipping schemes based on the rewetting of all degraded wetlands (ALL) and rewetting wetlands that only contain high-organic carbon stocks (high-*OCS*) (*Methods*; Supplementary Figure S3).

We find that of a total of 4.85 Mkm^2 of degraded wetlands until 2020, fewer than half (2.02 Mkm^2) were still emitting GHGs, and the remaining 2.83 Mkm^2 were completely degraded (Supplementary Figure S4). In the case of the latter, the soil carbon pool limits the duration for which GHGs are potentially emitted from ecosystems[36,37]. We then estimate that a widespread rewetting of degraded wetlands, with restoration rates of the same magnitude as the historical degradation rates, can potentially reduce GHG emissions by 248.7±154.6 Gt CO_2eq (ALL rewetting scenario) and 156.4±94.2 Gt CO_2eq (high-*OCS* scenario) by 2100 (Figure 4c, Extended Data Table 2). The latter contribution was mainly from freshwater marshes and floodplains (48.6%), and peatlands (38.2%). The reduction of emissions from peatlands is an average 0.75 Gt CO_2eq yr^{-1}, consistent with 0.5 Gt yr^{-1} reported by Evans *et al.*[24] based on the "optimal re-wetting" scenario in which 65% of peat is under cropland and grassland (0.77 Gt in 100% peat). The corresponding CO_2 reductions are 192.9±104.4 Gt (accounting for 77.6% of the sum of the three GHGs at 248.7 Gt CO_2eq) and 107.0±48.7 Gt (68.4%), respectively, for the two scenarios. Although the area proportion of high-*OCS* to ALL wetlands is only 42.9% (-0.92+2.92 Mkm^2 versus 1.34+2.92 Mkm^2, Supplementary Figure S4), the GHG emission reduction potential is as high as 62.9% (156.4 Gt CO_2eq versus 248.7 Gt CO_2eq), owing to the differences in the higher carbon density.

These projections are presumed to consider the effects of various types of wetlands and a changing climate. The duration of potential degradation related to GHG emissions from wetlands is constrained by the initial carbon pool and degradation rate (Equation 4, Supplementary Figure S5), which vary according to wetland type and the climate regime. However, in our extension of this assessment to the future, we assume the effect of climate change will be negligible on emission

rates, although there would be an unknown additional climate effect. We base this assumption on the similarity in GHG emissions rates between temperate and boreal regions for drained conditions (*WTL*-3; ≤-70cm) (Figures 2a-b and Extended Data Table 2). The similarity suggests emissions in cold regions would not change greatly with the magnitude of anticipated warming. Although the same comparison applied to the temperate versus tropical wetlands indicates a non-negligible impact of warming, the overall impact should be limited because of the low proportion of total emissions from temperate wetlands (4.6%; Extended Data Figure 7). In contrast, emissions of GHGs in the tropics would likely be sufficient to deplete the carbon pool prior to 2100 (Extended Data Figure 7a&d). Another issue of consideration is the effect that individual wetland categories would have on the effectiveness of the rewetting measures. However, there are consistent GHG exchange rates across various wetland categories (Supplementary Figure S6 a-f) that are similar to the sum exchange of GHGs across different climate regimes (e.g., *WTL*0, Figures 2a-c and Extended Data Table 2), although for which CO_2 and CH_4 fluxes vary significantly (Supplementary Figure S7 a-c).

A general limitation in our assessment stems from the natural WET index being produced at an intercontinental scale, rather than at a local scale[4,5]. This limitation prevents the development of a more detailed assessment of the GHG budgets associated with wetland degradation and/or restoration. In addition, we could not consider fire disturbances for wet versus dry conditions[38,39] or the response of substratum over one meter deep. Thus, our estimated GHG emissions from degraded wetlands may be conservative, and the GHG-reduction potential of rewetting programs is likely to be underestimated. Nevertheless, our estimated annual emissions from degraded wetlands for CO_2 and N_2O, or from whole natural freshwater wetlands for CH_4, are significantly

correlated with their respective annual growth rates in atmospheric concentration[40] during the past three decades ($P < 0.05$; Extended Data Figure 8, more details in *Methods* section: *Wetland GHG budgets and inter-annual atmospheric GHG growth rates*), supporting the utility of our method of integrating the natural WET index with the empirical GHG emission rates. Furthermore, the magnitudes of the estimated CO_2, CH_4, and N_2O emissions from the wetlands, equaling to 10.8±6.2%, 38.5±16.7%, and 30.5±19.4% respectively of the anthropogenic sources[12,41,42], are in line with the aforementioned correlations.

Despite uncertainties, we find that wetland rewetting is an effective nature-based solution to mitigate climate change. The rewetting ALL scenario and the high-*OCS* scenario require preserving or restoring 4.26 Mkm^2 and 2 Mkm^2 areas of degraded wetlands, respectively, compared with the business-as-usual scenario derived from historical trends (Supplementary Figure S4). The two rewetting scenarios can reduce GHG emissions by 583.8 $tCO_2eq\ ha^{-1}$ and 782 $tCO_2eq\ ha^{-1}$, respectively. The potential of GHG reduction from wetland restoration at this scale is higher than that from the rehabilitation of other types of ecosystems, for example, forest regrowth equivalent to 394.2 $tCO_2\ ha^{-1}$ across 6.78 Mkm^2 of afforestation under the 'maximum' scenario, or 504.3 $tCO_2\ ha^{-1}$ across 3.49 Mkm^2 under the 'national commitments' scenario[43]. At present, Indonesia, Europe, and North America have already shown the benefits of raising water tables by both artificial and natural means[44-47]. In cases where the water table is lowered by groundwater extraction, water conservancy measures may be needed to regulate water use—and the potential negative impacts of doing so should be balanced[48,49].

Conclusion

In conclusion, the non-linear thermal-wetness influence on wetland GHG fluxes, whereby a near-surface water table produces near-neutral GHG flux across broad temperature gradients, suggests that rewetting wetlands is an effective nature-based solution to mitigate climate change. A volume equivalent to ten percent of anthropogenic CO_2 emissions could be reduced through wetland restoration. By quantifying the impact of natural wetland area changes on multiple GHG budgets under several scenarios, we provide primary information for nature-based solutions predicated on wetland restoration for countries aiming to achieve net-zero emission targets[50]. Furthermore, we emphasize the enormous loss of organic matter and GHG emissions from over half of the global wetland ecosystems due to drying, as well as future emissions from these sources can be mitigated or even halved by rewetting wetlands to a near-surface water table.

Acknowledgments

We thank many individuals for measuring and providing *in-situ* GHG net fluxes from wetlands. **Funding**: This study was supported by the National Natural Science Foundation of China (grant no. 42071022), the start-up fund provided by the Southern University of Science and Technology (grant no. 29/Y01296122), and the High-level Special Funding of the Southern University of Science and Technology (grant no. G02296302). J.W. was in part supported by the Innovation and Technology Fund (funding support to State Key Laboratories in Hong Kong of Agrobiotechnology) of the HKSAR, China. D. C. was supported by Swedish National Strategic Research Programs: Biodiversity and Ecosystem Services in a Changing Climate (BECC) and ModElling the Regional and Global Earth system (MERGE). P.C. acknowledges support from the CLAND Convergence Institute 16-CONV-0003.

Author contributions

J.Z. and Z.Z. designed the research; J.Z. performed the analysis; J.Z., Z.Z. and A.D.Z. wrote the draft. All authors contributed to the interpretation of the results and the writing of the paper.

Correspondence and requests for materials should be addressed Z.Z. (zengzz@sustech.edu.cn).

Competing interests

The authors declare that they have no competing interests.

Figure Legends.

Figure 1. Water table level effects on global wetland net ecosystem exchange (NEE) and total greenhouse gas (GHG) emissions. (**a**) Relationship between NEE and sum of three GHGs (CO_2, CH_4, N_2O) net-flux in different WTLs, drawn from 174 site-year records that reported three greenhouse gases. (**b**) NEE, CH_4, N_2O and sum of three net fluxes for different WTL conditions. (**c-f**) Total and individual GHG fluxes for the 6 different WTLs considered. Points in each box are sampled from the original dataset (3,672 site-year records totally) with 1,000 bootstraps. Different letters in the boxes indicate significant differences ($P < 0.01$) between various WTLs based on nonparametric Wilcoxon signed-rank tests. Bold vertical lines show the median, boxes indicate the middle two quartiles, horizontal lines indicate the nonoutlier range. Note that X-axes have been truncated for enhanced readability.

Figure 2. Non-linear hydro-thermal influence on GHG exchange. Dependency of GHG emissions in boreal (**a**), temperate (**b**), and tropical (**c**) regions to water table level and climate. The "mean" groups (**d**) are calculated from equilateral weighted averages in each climate regime. Dots and shadows represent mean ± 1.96SEs. (**e-h**) Contribution ratios of NEE, CH_4, and N_2O to the sum of three GHGs net-flux in the three climatic regions and the mean.

Figure 3. Greenhouse gas (GHG) emissions from degraded wetlands under different scenarios. (**a**) Time-series of GHG emissions from degraded wetlands under three scenarios since 1950. The emissions are constrained by natural WET index and soil organic carbon pool. 'History trend' is history-derived scenario. 'Rewet (ALL)' and 'Rewet (High-OCS)' are based on the rewetting restoration of all and only high organic carbon stock wetlands, respectively. (**b**) GHG

net flux from degraded wetlands in main countries and continents over different periods. 'Others' refers to the sum of GHGs from countries that were not in the top ten of GHG emitters. 'EU', 'NA', 'SA', 'AS&OA', 'AF' are Europe, North America, South America, Asia and Oceania, and Africa, respectively.

Figure 4. Spatial pattern of the greenhouse gas emissions owing to wetland degradation (a, b) and reduction potential via rewetting wetlands (c). The GHG emissions under history-driven scenario in 1950-2020 (**a**) and under history-driven, business-as-usual scenario in 2021-2100 (**b**). (**c**) The reduction potential under rewetting all degraded wetland area scenario in 2021-2100.

References

1 Lindgren, A., Hugelius, G., Kuhry, P. Extensive loss of past permafrost carbon but a net accumulation into present-day soils. *Nature* **560**, 219–222 (2018).

2 Nichols, J. E., & Peteet D. M. 2019. Rapid expansion of northern peatlands and doubled estimate of carbon storage. *Nat. Geosci.* **12**, 917–921.

3 Bridgham, S. D. *et al*. The carbon balance of North American wetlands. *Wetlands* **26**, 889–916 (2006).

4 Dixon, M.J.R. *et al*. Tracking global change in ecosystem area: The wetland extent trends index. *Biol. Conserv.* **193**, 27–35 (2016).

5 Darrah S. E. *et al*. Improvements to the Wetland Extent Trends (WET) index as a tool for monitoring natural and human-made wetlands. *Ecol. Indic.* **99**, 294–298 (2019).

6 Asselen, S. *et al*. Drivers of wetland conversion: a global meta-analysis. *PloS One* **8**, e81292 (2013).

7 Davidson, N. C. How much wetland has the world lost? Long-term and recent trends in global wetland area. *Mar. Freshw. Res.* **65**, 934–941 (2014).

8 Galatowitsch, S. M. Natural and anthropogenic drivers of wetland change. In The *Wetland Book II: Distribution, Description, and Conservation* (*eds* Finlayson, C.M. *et al.*) pp. 359–367 (Springer, Netherlands, 2018).

9 Limpert, K. E. *et al*. Reducing emissions from degraded floodplain wetlands. *Front. Environ. Sci.* **8**, 1–18 (2020).

10 Laine, J. *et al*. Effect of water-level drawdown on global climatic warming: Northern peatlands. *AMBIO* **25**, 179–184 (1996).

11 Ise, T. *et al*. High sensitivity of peat decomposition to climate change through water-table feedback. *Nat. Geosci.* **1**, 763–766 (2008).

12 Saunois, M. *et al*. The global methane budget 2000–2017. *Earth. Syst. Sci. Data* **12**, 1561–1623 (2020).

13 Leifeld, J. *et al*. Intact and managed peatland soils as a source and sink of GHGs from 1850 to 2100. *Nat. Clim. Chang.* **9**, 945–947 (2019).

14 Günther, A. *et al*. Prompt rewetting of drained peatlands reduces climate warming despite methane emissions. *Nat. Commun.* **11**, 1644 (2020).

15 Hooijer, A. *et al*. Subsidence and carbon loss in drained tropical peatlands. *Biogeoscience* **9**, 1053–1071 (2012).

16 Prananto, J. A. *et al*. Drainage increases CO_2 and N_2O emissions from tropical peat soils. *Glob. Chang. Biol.* **26**, 4583–4600 (2020).

17 Jauhiainen, J. *et al*. Carbon dioxide and methane fluxes in drained tropical peat before and after hydrological restoration. *Ecology* **89**, 3503–3514 (2008).

18 Bridgham, S. D. *et al*. Methane emissions from wetlands: biogeochemical, microbial, and modeling perspectives from local to global scales. *Glob. Chang. Biol.* **19**, 1325–1346 (2013).

19 Schuldt, R. *et al*. Modelling Holocene carbon accumulation and methane emissions of boreal wetlands – an Earth system model approach. *Biogeosciences* **10**, 1659–1674 (2012).

20 McNicol, G. *et al*. Effects of seasonality, transport pathway, and spatial structure on greenhouse gas fluxes in a restored wetland. *Glob. Chang. Biol.* **23**, 2768–2782 (2017).

21 Yu, K. *et al*. Redox window with minimum global warming potential contribution from rice soils. *Soil Sci. Soc. Am. J.* **68**, 2086–2091 (2004).

22 Huang, Y., Ciais, P., Luo, Y. *et al*. Tradeoff of CO_2 and CH_4 emissions from global peatlands under water-table drawdown. *Nat. Clim. Chang.* **11**, 618–622 (2021).

23 Ojanen, P., & Minkkinen K. Rewetting offers rapid climate benefits for tropical and agricultural peatlands but not for forestry‐drained peatlands. *Glob. Biogeochem. Cycles* **34**, e2019GB006503 (2020).

24 Evans, C.D. *et al*. Overriding water table control on managed peatland greenhouse gas emissions. *Nature* **593**, 548–552 (2021).

25 Strack, M., Keith, A. M., & Xu, B. Growing season carbon dioxide and methane exchange at a restored peatland on the Western Boreal Plain. *Ecol. Eng.* **64**, 231–239 (2014).

26 Karki, S., Elsgaard, L., Kandel, T. P. *et al*. Carbon balance of rewetted and drained peat soils used for biomass production: a mesocosm study. *Gcb. Bioenergy* **8**, 969–980 (2016).

27 Whiting, G. J., & Chanton, J. P. Greenhouse carbon balance of wetlands: Methane emission versus carbon sequestration. *Tellus B Chem. Phys. Meteorol.* **53**, 521–528 (2001).

28 Moore, T. R. *et al*. A multi-year record of methane flux at the Mer Bleue Bog, Southern Canada. *Ecosystems* **14**, 646–657 (2011).

29 Zhu, X. *et al*. Ammonia oxidation pathways and nitrifier denitrification are significant sources of N_2O and NO under low oxygen availability. *Proc. Natl. Acad. Sci. U.S.A.* **110**, 6328–6333 (2013).

30 Cole, J. J. *et al*. Plumbing the global carbon cycle: Integrating inland waters into the terrestrial carbon budget. *Ecosystems* **10**, 171–184 (2007).

31 Holgerson, M. A., & Raymond, P. A. Large contribution to inland water CO_2 and CH_4 emissions from very small ponds. *Nat. Geosci.* **9**, 222–226 (2016).

32 Raymond, P. A. *et al*. Global carbon dioxide emissions from inland waters. *Nature* **503**, 355–359 (2013).

33 Rosentreter, J. A. *et al*. Half of global methane emissions come from highly variable aquatic ecosystem sources. *Nat. Geosci.* **14**, 225–230 (2021).

34 Lehner, B., & Döll, P. Development and validation of a global database of lakes, reservoirs and wetlands. *J. Hydrol.* **296**, 1–22 (2004).

35 Schuur, E. A. *et al*. The effect of permafrost thaw on old carbon release and net carbon exchange from tundra. *Nature* **459**, 556–559 (2009).

36 Delgado-Baquerizo, M. *et al*. Climate legacies drive global soil carbon stocks in terrestrial ecosystems. *Sci. Adv.* **3**, e1602008 (2017).

37 Hengl, T. *et al*. SoilGrids250m: Global gridded soil information based on machine learning. *PLoS One* **12**, e0169748 (2017).

38 Walker, X. J. *et al*. Increasing wildfires threaten historic carbon sink of boreal forest soils. *Nature* **572**, 520–523 (2019).

39 Baird, A. J. *et al*. Validity of Managing Peatlands with Fire. *Nat. Geosci.* **12**, 884–85 (2019).

40 Our World In Data: Atmospheric concentrations (*eds* Ritchie, H., & Roser, M.). https://ourworldindata.org/atmospheric-concentrations

41 P. Friedlingstein *et al*. Global Carbon Budget 2019. *Earth Syst. Sci. Data* **11**, 1783–1838 (2019).

42 Tian, H. *et al*. A comprehensive quantification of global nitrous oxide sources and sinks. *Nature* **586**, 248–256 (2020).

43 Cook-Patton, S. C. *et al*. Mapping carbon accumulation potential from global natural forest regrowth. *Nature* **585**, 545–550 (2020).

44 Jaenicke, J. *et al*. Planning hydrological restoration of peatlands in Indonesia to mitigate carbon dioxide emissions. *Mitig. Adapt. Strateg. Glob. Chang.* **15**, 223–239 (2010).

45 Wohl, E. Landscape-scale carbon storage associated with beaver dams. *Geophys. Res. Lett.* **40**, 3631–3636 (2013).

46 Law, A. *et al*. Using ecosystem engineers as tools in habitat restoration and rewilding: Beaver and wetlands. *Sci. Total. Environ.* **605**–**606**, 1021–1030 (2017).

47 Brown, L. E. *et al*. Macroinvertebrate community assembly in pools created during peatland restoration. *Sci. Total Environ.* **569**, 361–72 (2016).

48 Finlayson, C. M., & Rea, N. Reasons for the loss and degradation of Australian wetlands. *Wetl. Ecol. Manag.* **7**, 1–11 (1999).

49 Liu, J., *et al*. Water conservancy projects in China: Achievements, challenges and way forward. *Glob. Environ. Change* **23**, 633–643 (2013).

50 Rogelj, J. *et al*. in *Global Warming of 1.5°C: An IPCC Special Report on the Impacts of Global Warming of 1.5°C Above Pre-industrial Levels and Related Global Greenhouse Gas Emission Pathways, in the Context of Strengthening the Global Response to the Threat of Climate Change, Sustainable Development, and Efforts to Eradicate Poverty*

(*eds* Flato, G., Fuglestvedt, J., Mrabet, R. & Schaefer, R.) Ch. 2, 93–174 (IPCC/WMO, 2018).

Methods

In-situ database of GHGs

We searched for literature through the *Web of Science* using the following strings: (greenhouse gases flux (greenhouse gas* OR GHG* OR carbon dioxide OR CO_2 OR net ecosystem productivity* OR NEP OR net ecosystem exchange* OR NEE OR carbon OR methane OR CH_4 OR nitrous oxide OR N_2O OR flux* OR emission* OR global warming potential OR GWP) OR (degradation* OR decline*) and wetland (wetland* OR water* OR peatland* OR bog* OR fen* OR swamp* OR mire* OR soil* OR river* OR paddy OR pool* OR floodplain* OR reservoir* OR coastal* OR saltmarsh*)). The search returned 33,835 papers after excluding those in irrelevant fields. After screening the manuscripts to ensure that the records contained measured data from field monitoring projects, 2,563 papers were manually selected, from which we read to extract the following information: 1) Gas sample collection methods (this content may be missing, e.g., eddy covariance method (EC) measured CO_2 and/or CH_4 fluxes without collecting gas samples) and measurement techniques; 2) Time intervals and the duration of sample collection. We specified that the monitoring span during the growing season should be at least three months in temperate regions; 3) Detailed site information, in particular geographic coordinates or maps that could be georeferenced, as well as topography, ecosystem type, plant species, and soil carbon features. After screening, we obtained 504 papers with valid data (Supplementary Data S1). Parts of those data were extracted from figures by GetData Graph (version 2.26).

Record details

We constructed a GHG net-flux database consisting of 3,704 site-years (1,875 sites) for locations situated between 81°48' N and 78°01' S (Extended Data Figure 1a-c) across all the continents, but

436 mainly in Asia, Europe, and North America. The sample collection method and measurement
437 technique used in these field monitoring projects usually depended on the type of wetland and
438 associated environmental conditions. Common collection methods included the static chamber
439 method[51], dynamic chamber method[52] and floating chamber method[53]. Common measurement
440 techniques involve the use of infrared gas analyzer (IRGA), and the combination of gas
441 chromatography (GC) with physical model methods [e.g., EC[54], CO_2/CH_4-diffusivity formula[53],
442 oxygen diffusivity formula[55], or chlorophyll-dissolved oxygen model[56]]. We assume that these
443 GHG exchange rates from peer-reviewed papers based on different sampling methods are of
444 equivalent accuracy, although there may be differences in precision.
445
446 Nomenclature corresponding to the exchange of CO_2 between the ecosystem and the atmosphere
447 used in various methods is diverse. The EC method generally uses a net ecosystem exchange (*NEE*)
448 to characterize the flux, while the chamber method adopts the net ecosystem production (*NEP*)
449 approach. While a few sites measure both vertical exchange and transverse flow of GHGs[2,30], most
450 of the sites only report the measurements of vertical fluxes. Consequently, the data sets we built
451 describe the fluxes in the vertical direction. In cases where data were reported for the growing
452 seasons (Extended Data Figure 1b), we filled in the missing data using linear regression, based on
453 complete data containing both growing and annual records (Supplementary Table S1). There was
454 no significant interaction effect of climate regimes on the slope, and only a subtle effect on the
455 intercept of the NEE regression equation for temperate zones. Therefore, we chose linear
456 regression equations that did not take into account the interaction of the climate regimes.
457
458 We used NEE to describe the net vertical exchange capacity:

$$NEE = Re - GPP = Rh - NPP \quad (1)$$

where *Re* is ecosystem respiration, *GPP* is gross primary productivity, *Rh* is heterotrophic respiration, and *NPP* is net primary productivity. Positive values of *NEE* indicate carbon loss via CO_2 emission to the atmosphere, whereas negative values indicate carbon gain because CO_2 is retained/stored in the ecosystem.

Building on equation (1), we calculated the total flux of three GHGs, carbon dioxide, methane, and nitrous oxide as

$$GHGs = NEE + 34CH_4 + 298N_2O \quad (2)$$

where CO_2 is substituted by *NEE*. Units for all terms are kg CO_2eq ha^{-1} yr^{-1}; the weights 34 and 298 are global warming potential (GWP) for CH_4 and N_2O to CO_2 equivalent by weights on a 100-year perspective with feedbacks considered[57], respectively.

Uncertainty is represented by incorporating 95% confidence intervals (CI):

$$GHGs\_CI = NEE\_CI + 34CH_4\_CI + 298N_2O\_CI \quad (3)$$

where the CI of three GHGs on the right side of these originate from within groups, whereby uncertainties in empirical GHGs emission rates are obtained for 18 groups, including 6 WTL categories × 3 climatic zones.

Wetland categories

The majority of the records collected in this study were measured in natural wetlands, including bogs, fens, mires, swamps, marshes, floodplains, etc.; we also considered water bodies as extensions. We distinguished peatlands from non-peatlands based on the soil organic layer

thickness (i.e. peatlands ≥ 40 cm)[58], in order to explore the influence of soil organic matter on multi-GHG fluxes. We divided all sites into six water categories based on either the water level (flooded) or the water table height (non-flooded) relative to the surface (water-table/level, *WTL*), for three climatic regions (tropical, temperate, boreal, or high-altitude areas; using 4 ºC and 17 ºC of multiyear-average annual temperature as thresholds)[59]. We also treat water level as a continuous variable in Extended Data Figure 2, using 2,318 site-year records that reported exact water levels. Unfortunately, reports with high quality water level records from the tropics accounted for only 7% of the total. As such, the trend for the tropics using the continuous variable approach has more uncertainty for other climates. Therefore, we segmented all the water table/level data. The *WTL* classes were separated by mean water table/level during the growing season due to the discontinuity of the reported hydrological records during wintertime at most sites. Six classes are divided from *WTL*-3 to *WTL*2: ≤ -70; -70 to -50; -50 to -30; -30 to -5; -5 to 40; > 40 cm. Positive numbers indicate that the water level is above the surface. This classification is based on the empirical water level critical value of the soil moisture conditions, ranging from drought to moist to near-saturated to oversaturated[60]. We used an empirical value of 40 cm water level as a threshold to classify high water levels as they usually inhibit the establishment of emergent plants. We defined the start/end of a growing season as the time when the daily mean temperature for five continuous days was above/below 5 ºC for the first time[61].

We extracted the global natural wetland map from the Global Lakes and Wetlands Database level 3 (GLWD-3, classes 4, 5, 8-12)[34], which provides reliable areas of global wetlands, with tropical peatlands distinguished[62-64]. Its classification of wetlands also agrees with most records in the literature we selected. Gridded long-term mean annual air temperature was calculated using the

monthly data from the latest ECMWF reanalysis (ERA5 (ref. 66)) for 1978-2018. Gridded wetland soil organic carbon stock (*OCS*) was obtained from SoilGrids[37], which indicates that natural freshwater wetlands cover 7.66 million km^2 and store 329.5 Gt C in the upper one meter of the soil (Extended Data Table 2). The proportion of wetlands in boreal, temperate, and tropical regions are 45.8%, 10.8%, and 43.4%, respectively.

Dynamic area of wetlands under three scenarios

Means and 95% CIs of GHG net-fluxes in *WTL*-3 (≤-70 cm) for different climatic zones were used as the emission potential from degraded wetlands (Extended Data Figure 2b, Extended Data Table 1). We employed the mean OCS for each wetland category in each country as a constraint, and then calculated the duration potential (*DP*, Supplementary Figure S5) of soil carbon efflux from degraded wetlands for 21 wetland types (3 climate zones (i.e., tropical, temperate, boreal or high-altitude zones) × 7 wetland category groups (including bog, fen, mire, swamp forest, flooded forest, freshwater marsh, floodplain) at the national scale as follows:

$$DP = (OCS - OCSt) / NEE,\ DP \geq 1 \quad (4)$$

We used an OCS_t (threshold) of 50 t ha^{-1} (ref. 36), after which an ecosystem has no potential for net CO_2 emission from the soil layer. To avoid double-counting, we did not consider the other GHG exchanges of completely degraded wetlands, which have been definitely converted into farmland or pasture, etc. These are included in the estimate of land use and agriculture emissions by the Carbon Budget Project[35] and FAO[66].

We rebuilt the historical trend and predicted the future wetland degradation rate at the continental scale using the natural Wetland Extent Trends (WET) index[4,5] for 1970-2015 (Supplementary

Figure S2). The WET index is a multi-source composite index to represent the proportion of wetland degradation or construction during 1970-2015 (Europe in 1970–2013). We extended the time series to 1950-1969 and 2016-2100 from regressions using the 1970-1990 and 2000-2015 data (Europe predicted by 2000-2013 due to the data restriction); these calculations are for the history-derived scenario (history-derived). We used two wetland restoration benchmarks: one considered all wetlands (ALL) and the other only involved the high-*OCS* wetlands (high-*OCS*) (Supplementary Figure S3). High-*OCS* wetlands were determined as those with a duration potential > 80 years. The total area of high-*OCS* wetlands worldwide is 3.29 M km^2, of which 34.5% are degraded. The ALL and high-*OCS* scenarios were both grounded on the assumption that the restoration rate of those degraded wetlands would exceed that of the historical degradation rate in all continents by 2030. Thus, prior to 2030, restoration proceeded at a rate equivalent to the absolute value of the degradation rate during 2000-2015 (2000-2013 for Europe). The increase stopped when the natural WET index recovered to the level in 1950 (Supplementary Figure S2).

A *completely degraded* wetland was defined as having no potential for soil carbon loss, and *the wetland during degradation* was defined as those with continuous loss of carbon and nitrogen (*WTL*-3) to the atmosphere. The remainder were classified as *initial & rewetted* wetlands. The component of dynamic wetland area under three scenarios in Supplementary Figure S4 shows the trends of the area in three conditions during 1950-2100 (more details in Supplementary Data S1).

Supporting calculations

Empirical GHG exchange rates

Based on the empirical values (*WTL*0, *WTL*2) in the relationship between *WTL* and GHG emissions across different temperature regimes (Extended Data Table 1), we calculated that the GHG emissions from global water bodies (lakes & reservoirs) are $1.0^{+0.93}_{-0.93}$ Gt CO_2 and $127.5^{+49.4}_{-49.4}$ Tg CH_4, and CH_4 emissions from natural freshwater wetlands is $144.4^{+67.9}_{-67.9}$ Tg. These results agree with previous reports, whose corresponding values are $1.2^{+1.91}_{-0.95}$ Gt CO_2 (ref. 32), and 175.2^{+81}_{-81} Tg CH_4 (ref. 33), $148.6^{+15.2}_{-15.2}$ Tg CH_4 (ref. 12) respectively (Supplementary Figure S1).

The GHG emissions from boreal and temperate regimes in *WTL*-3 ($\leqslant$ -70 cm) are 19.7 and 11.2 $tCO_2eq\ ha^{-1}\ yr^{-1}$ respectively, which are similar to the drained-*induced* GHG emission factor 16.1 $tCO_2eq\ ha^{-1}\ yr^{-1}$ for boreal & temperate in Leifeld *et al.*[13]. Furthermore, the CO_2 emission rate in the boreal regime is $13.43^{+5.49}_{-5.59}$ $tCO_2\ ha^{-1}\ yr^{-1}$, which is similar to the cultivated northern peatlands emission factor $13.2^{+0.73}_{-1.1}$ $tCO_2\ ha^{-1}\ yr^{-1}$ in Qiu *et al.*[67] from a process-based land surface model.

Estimation of GHG emissions from degraded wetlands under three scenarios

We estimated the changes of GHG emissions driven by the degraded wetland area and *OCS* in various wetland types under three scenarios (history-derived, ALL, and high-*OCS*) and across different scales. At the national scale, countries with large *OCS* were the dominant emitters of GHGs, mainly CO_2. The top 10 GHG emitting countries contributed to 79.6% of the total emissions in the period 1950-2020 (Figure 3, Extended Data Figures 5-6). At the continental scale, the top two continents, South America (SA) and North America (NA); accounted for 37.7% and 22.7%, respectively. With respect to climate regime, countries in tropical and boreal regions occupied 55.4% and 39.7% due to their potent outflow and high *OCS*.

In the scenario for which the historical trend continues during the period 2021-2100 (history-derived scenario), the wetland degradation area will increase to 74.0% by the end of the 21st century, and the induced GHGs will be enlarged by 1.48 times to 407.9 Gt (Figures 3-4, Extended Data Table 2). In addition, the present geographical pattern of outflow will change: in tropical regions, along with the loss of most soil *OCS*, emissions will reduce from 155.2 Gt to 99.1 Gt, while boreal regions will become the dominant emission source, increasing from 107.9 Gt to 290.0 Gt (39.0% to 71.1%).

Under the wetland restoration scenarios for which rewetting occurs for all degraded wetlands (ALL) or only high-*OCS* degraded wetlands (high-*OCS*), the total GHG emissions could reduce by 248.7 or 156.4 Gt, respectively. The emission reduction mainly results from the reduced GHG emissions over boreal regions. In the high-*OCS* scenario, CO_2 accounted for 79.2% of the global total GHG emissions (Extended Data Table 2), higher than that in the ALL scenario (71.2%) and the history-derived scenario (75.0%). This finding results from a large percentage of the degraded low-*OCS* wetlands being distributed in the tropics but is not restored in the high-*OCS* scenario, where the tropics contribute to the largest portion of global CO_2 emissions with the highest CO_2 outflow potential in the per area (Figure 2, Extended Data Figure 5).

All of the above conclusions are based on a GWP for CH_4 of 34-fold that of CO_2 by weights over a 100-year period. We have also supplemented our assessment of emissions and reductions with a 28-fold GWP or a 45-fold sustained GWP (sGWP)[68,69]. The results of GHG emission estimation show differences of +0.23% and -0.43%, respectively, compared to the history-derived scenario

591 with a 34-fold base in 1950-2100. The estimation of GHG emission reduction change in 0.37%
592 and -0.67% under the rewetting all scenario, 0.22% and -0.41% under the rewetting high-*OCS*
593 scenario in 2020-2100, respectively.

594

595 *Wetland GHG budgets and inter-annual atmospheric GHG growth rates*

596 There are significant correlations between annual growth rates in atmospheric concentrations and
597 changes in the wetland-induced flux for CO_2, CH_4, and N_2O in 1979-2018, respectively (P <0.05;
598 Extended Data Figure 8a-i, N_2O is in 1979-2016). The sum of N_2O emissions from degraded
599 wetland and FAO agriculture-total[66] also is also significantly correlated with atmospheric
600 concentration growth rates (P < 0.05; note that N_2O data exclude two early extremes values in
601 1979 and 1982). Emissions of CO_2 from degraded wetlands are highly consistent with those from
602 land-use changes in the Carbon Budget Project[35], with the former being ~81.4% (ranging from
603 64.5% to 97.5%) of the latter across 30 years. The net CH_4 emissions from both degraded and
604 initial & rewetted wetlands exhibited a downward trend during 1979-2018. This change may have
605 contributed to the decline of atmospheric methane growth rates before 2005, which is reversed by
606 the increase of emissions from other major sources (e.g. agriculture[68]) since then. The evident
607 correlations between wetland budgets and atmospheric growth of three key GHGs indicate the
608 non-negligible impact of wetland degradation. Indeed, CO_2, CH_4, and N_2O emissions from
609 wetlands were equal to 10.8±6.2%, 38.5±16.7%, and 30.5±19.4% of those from anthropogenic
610 sources[12,41,42], which are similar to their contribution of 19%, 21% and 34% of the variation in
611 atmospheric concentrations during 1979-2018 (Extended Data Figure 8).

612

Uncertainties

Wetland area

Although many global wetland area products using diverse classification rules have been released[34,70-75], uncertainty remains in wetland characterizations and distribution worldwide. In particular, human-made wetlands have been increasing greatly in recent years, and natural wetlands continue to degrade[4,5,76]. The natural wetland classes (i.e., bog, fen, mire, swamp/flooded forest, freshwater marsh, floodplain) of GLWD-3 were built from the following three datasets in the 1990s: ArcWorld[77], DCW[78], and WCMC[79]. We conservatively considered the area of wetlands in GLWD-3 as the background value in 1990. The GLWD-3 did not include wetlands smaller than 0.1 km^2; however, this threshold ensured that the hydrologic features and biogeochemical processes of degraded wetlands can be restored to their initial states in a short term[80].

Degradation trend of natural wetlands

Many countries lack baseline wetland inventories that allow us to accurately track the lengthy and complex degradation of natural wetlands[81]. The WET index represents area change based on over 2,000 wetland area records in long-term time series from six regions, and distinguishes between human-made and natural wetland changes from 1970 to 2015. Given the differences between natural and artificial wetlands in the basal features (e.g., OCS, hydrologic features) and disturbance (e.g., artificial landscape, artificial nitrogen input), we only considered natural wetlands, via down-scaling the natural WET index from six continents to countries and/or regions. Therefore, additional surveys and remote sensing data would provide for a more accurate assessment at a finer scale in the future.

According to the WET index, the degraded wetland areas were 4.85 Mkm^2 for 1950-2020 (46.22% of the global natural wetlands). Under a history-derived, business-as-usual scenario for the future, we projected that continued wetland degradation will reach 7.76 Mkm^2 (74.0%) by the end of the 2021-2100 period. Note that these overall estimates include not only those wetlands degraded by land-use change (e.g., reclamation, draining), but also by other factors affecting the hydrological characteristics of wetlands (desiccation)[82]. For example, the peat loss to extraction or farming in Europe accounts for only 11% of European peatlands[67], but the water levels in another 50% of European peatlands are also declining, causing degradation[83].

Wetland categories

Empirical parameter generalization is based on the premise that there is no difference in emission potential across various wetland categories. Indeed, we found that, in the *WTL*0 group where GHG emissions are close to neutral (Figure 2, Extended Data Table 1), there is almost no significant difference in GHG emissions among the main wetland categories both for tropical and temperate regimes (Supplementary Figure S6). However, because of the lack of various types of wetlands in boreal regions (dominated by peatlands), we did not test the differences in GHG emissions across diverse categories for boreal climates. In the *WTL*-3 group, due to the lack of various wetland categories for comparison, we used the *OCS* to calculate the duration potential, which is further used to constrain the empirical parameter generalization for the estimate of the potential GHG emissions from degraded wetlands (see Equation 4).

Data availability

GLDW dataset is available at http://www.wwfus.org/science/data.cfm. Soilgrids dataset is available at https://soilgrids.org. ECMWF reanalysis climate data is available at https://cds.climate.copernicus.eu/#!/home. FAOSTAT emissions database is available at http://www.fao.org/faostat/en/#data/GT. Atmospheric concentrations data is available at https://ourworldindata.org/atmospheric-concentrations. All GHGs data is available in the main text or the supplementary materials. The database of global, in-situ, GHG exchange information for wetlands, drawn from 3,704 site-year records is summarized in Supplementary Data 1.

Code availability

The scripts used to generate all the results are MATLAB (R2018a), R-4.1.0, Python 2.7 based on arcpy. Analysis scripts are available at: https://github.com/XiaoBai0417/Multi-greenhouse-gas-assessments.

References

51 Svensson, B. H., & Rosswall, T. In situ methane production from acid peat in plant communities with different moisture regimes in a subarctic mire. *Oikos* **43**, 341–350 (1984).

52 Waddington, J. M., & Roulet, N. T. Atmosphere-wetland carbon exchanges: Scale dependency of CO_2 and CH_4 exchange on the developmental topography of a peatland. *Glob. Biogeochem. Cycles* **10**, 233–245 (1996).

53 Kling, G. W. *et al*. The flux of CO_2 and CH_4 from lakes and rivers in arctic Alaska. *Hydrobiologia* **240**, 23–36 (1992).

54 Humphreys, E. R. *et al*. Two bogs in the Canadian Hudson bay lowlands and a temperate bog reveal similar annual net ecosystem exchange of CO_2. *Arct. Antarct. Al. Res.* **46**, 103–113 (2014).

55 Caffrey, J. M. Factors controlling net ecosystem metabolism in *U.S.* estuaries. *Estuaries* **27**, 90–101 (2004).

56 Roberts, B. J. *et al*. Multiple scales of temporal variability in ecosystem metabolism rates: Results from 2 years of continuous monitoring in a forested headwater stream. *Ecosystems* **10**, 588–606 (2007).

57 Myhre, G. *et al*. Anthropogenic and Natural Radiative Forcing. In *Climate Change 2013: The Physical Science Basis. Contribution of Working Group I to the Fifth Assessment Report of the Intergovernmental Panel on Climate Change* (*eds* Stocker, T.F. *et al*.) pp.710–714 (Cambridge Univ. Press, 2013).

58 Glenn, A. J. *et al*. Comparison of net ecosystem CO_2 exchange in two peatlands in western Canada with contrasting dominant vegetation, *Sphagnum* and *Carex*. *Agric. For. Meteorol.* **140**, 115–135 (2006).

59 Bond-Lamberty, B., & Thomson, A. Temperature-associated increases in the global soil respiration record. *Nature* **464**, 579–582 (2010).

60 Zhao, J, Malone, SL, Oberbauer, SF. *et al*. Intensified inundation shifts a freshwater wetland from a CO_2 sink to a source. *Glob Change Biol.* **25**: 3319–3333 (2019).

61 Peichl, M. *et al*. A 12-year record reveals pre-growing season temperature and water table level threshold effects on the net carbon dioxide exchange in a boreal fen. *Environ. Res. Lett.* **9**, 55006 (2014).

62 Peng, Z. & Peng, G. Suitability mapping of global wetland areas and validation with remotely sensed data. *Sci. China Earth Sci.* **57**, 2883–2892 (2014).

63 Zhang, B. *et al*. Methane emissions from global wetlands: An assessment of the uncertainty associated with various wetland extent data sets. *Atmos. Environ.* **165**, 310–321 (2017).

64 Gumbricht, T. *et al*. An expert system model for mapping tropical wetlands and peatlands reveals South America as the largest contributor. *Glob. Chang. Biol.* **23**, 3581–3599 (2017).

65 European Centre for Medium-Range Weather Forecasts (ECMWF), ERA5 monthly averaged data on pressure levels from 1979 to present (2020). doi: 10.24381/cds.6860a573

66 FAO, 2020. FAOSTAT Emissions Database, Agriculture, Agriculture Total. http://www.fao.org/faostat/en/#data/GT

67 Qiu, C. *et al*. Large historical carbon emissions from cultivated northern peatlands. *Sci. Adv.* **7**, eabf1332 (2021).

68 Frolking, S., Roulet, N. and Fuglestvedt. J. How northern peatlands influence the earth's radiative budget: Sustained methane emission versus sustained carbon sequestration. *J. Geophys. Res. Biogeo.* **111**: G01008 (2006).

69 Neubauer, S. C., and J. P. Megonigal. Moving beyond global warming potentials to quantify the climatic role of ecosystems. *Ecosystems* **18**:1000-1013 (2015).

70 Matthews, E., & Fung, I. Methane emission from natural wetlands: global distribution, area, and environmental characteristics of sources. *Glob. Biogeochem. Cycles* **1**, 61–86 (1987).

71 Kaplan, J.O. A composite map of global wetland distribution at 0.5 degree resolution (2007); http://arve.epfl.ch/pub/wetlands/index.html.

72 Papa, F. et al. Interannual variability of surface water extent at the global scale, 1993–2004. *J. Geophys. Res. Atmos.* **115**, D12111 (2010).

73 Junk, W.J. *et al*. Current state of knowledge regarding the world's wetlands and their future under global climate change: a synthesis. *Aquat. Sci.* **75**, 151–167 (2013).

74 Schroeder, R. *et al*. Development and evaluation of a multi-year fractional surface water data set derived from active/passive microwave remote sensing data. *Remote Sens.* **7**, 16688–16732 (2015).

75 Vanessa, R. *et al*. A Global Assessment of inland wetland conservation status. *Bioscience* **6**, 523–533 (2017).

76 Davidson, N. *et al*. Global extent and distribution of wetlands: trends and issues. *Mar. Freshw. Res.* **69**, 620-627 (2018).

77 Environmental Systems Research Institute (ESRI): ArcWorld 1:3 Mio. Continental Coverage. Redlands, CA. Data obtained on CD (1992). http://www.oceansatlas.org/subtopic/en/c/593/

78 Environmental Systems Research Institute (ESRI): Digital Chart of the World 1:1 Mio. Redlands, CA. Data obtained on 4 CDs (1993). http://www.nlh.no/ikf/gis/dcw/

79 WCMC (World Conservation Monitoring Centre): Wetlands in Danger, P. Dugan, Ed. (1993). https://www.arcgis.com/home/item.html?id=105a402642e146eaa665315279a322d1

80 Moreno-Mateos, D. *et al*. Structural and functional loss in restored wetland ecosystems. *PLoS Biol.* **10**, e1001247 (2012).

81 Ramsar Convention Secretariat. Ramsar COP12 DOC.8. Report of the Secretary General to COP12 on the implementation of the Convention. (Ramsar Convention Secretariat: Gland, Switzerland.) (2015).

82 Page, S. E. *et al*. Peatlands and global change: response and resilience. *Annu. Rev. Environ. Resour.* **41**, 35–57 (2016).

83 Swindles G. T. *et al*. Widespread drying of European peatlands in recent centuries. *Nat. Geosci.* **12**, 922–928 (2019).

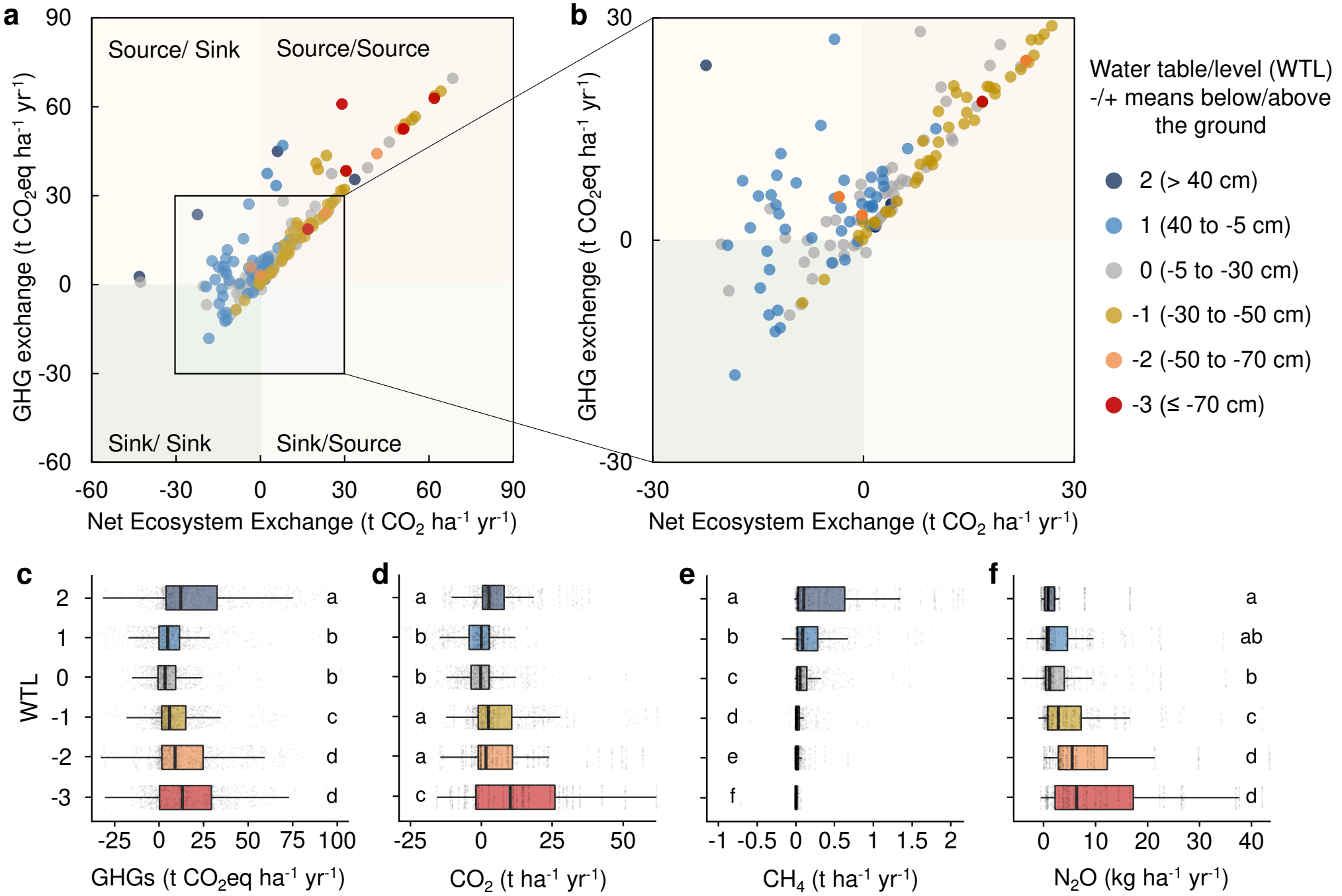
a
b
Source/ Sink
Source/Source
Sink/ Sink
Sink/Source
GHG exchange (t CO2eq ha-1 yr-1)
Net Ecosystem Exchange (t CO2 ha-1 yr-1)
GHG exchenge (t CO2eq ha-1 yr-1)
Net Ecosystem Exchange (t CO2 ha-1 yr-1)
Water table/level (WTL)
-/+ means below/above
the ground
2 (> 40 cm)
1 (40 to -5 cm)
0 (-5 to -30 cm)
-1 (-30 to -50 cm)
-2 (-50 to -70 cm)
-3 (≤ -70 cm)
c
d
e
f
WTL
GHGs (t CO2eq ha-1 yr-1)
CO2 (t ha-1 yr-1)
CH4 (t ha-1 yr-1)
N2O (kg ha-1 yr-1)

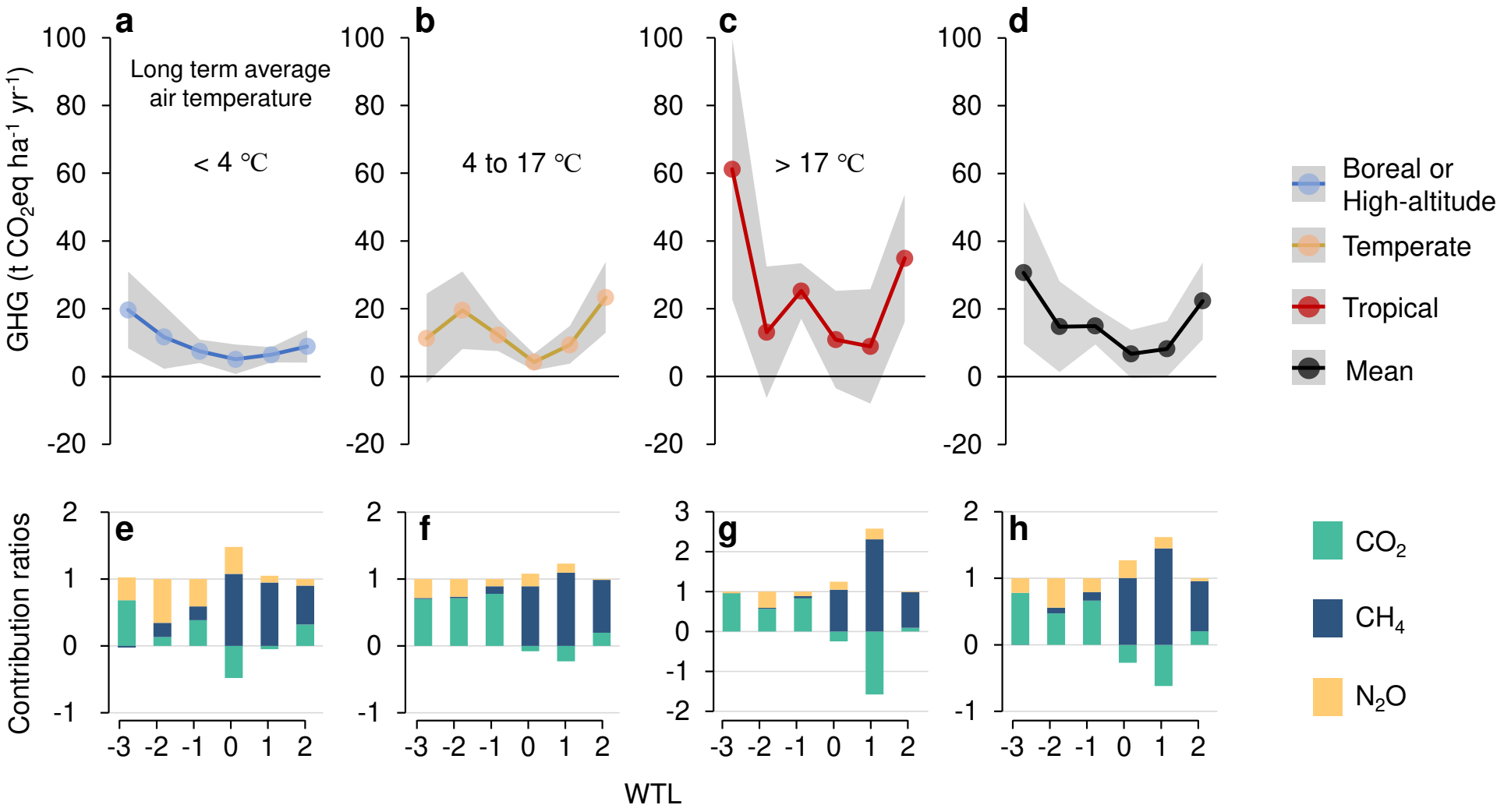
a
b
c
d
Long term average air temperature
< 4 ℃
4 to 17 ℃
> 17 ℃
GHG (t CO2eq ha-1 yr-1)
100
80
60
40
20
0
-20
Boreal or High-altitude
Temperate
Tropical
Mean
e
f
g
h
Contribution ratios
CO2
CH4
N2O
-3 -2 -1 0 1 2
WTL

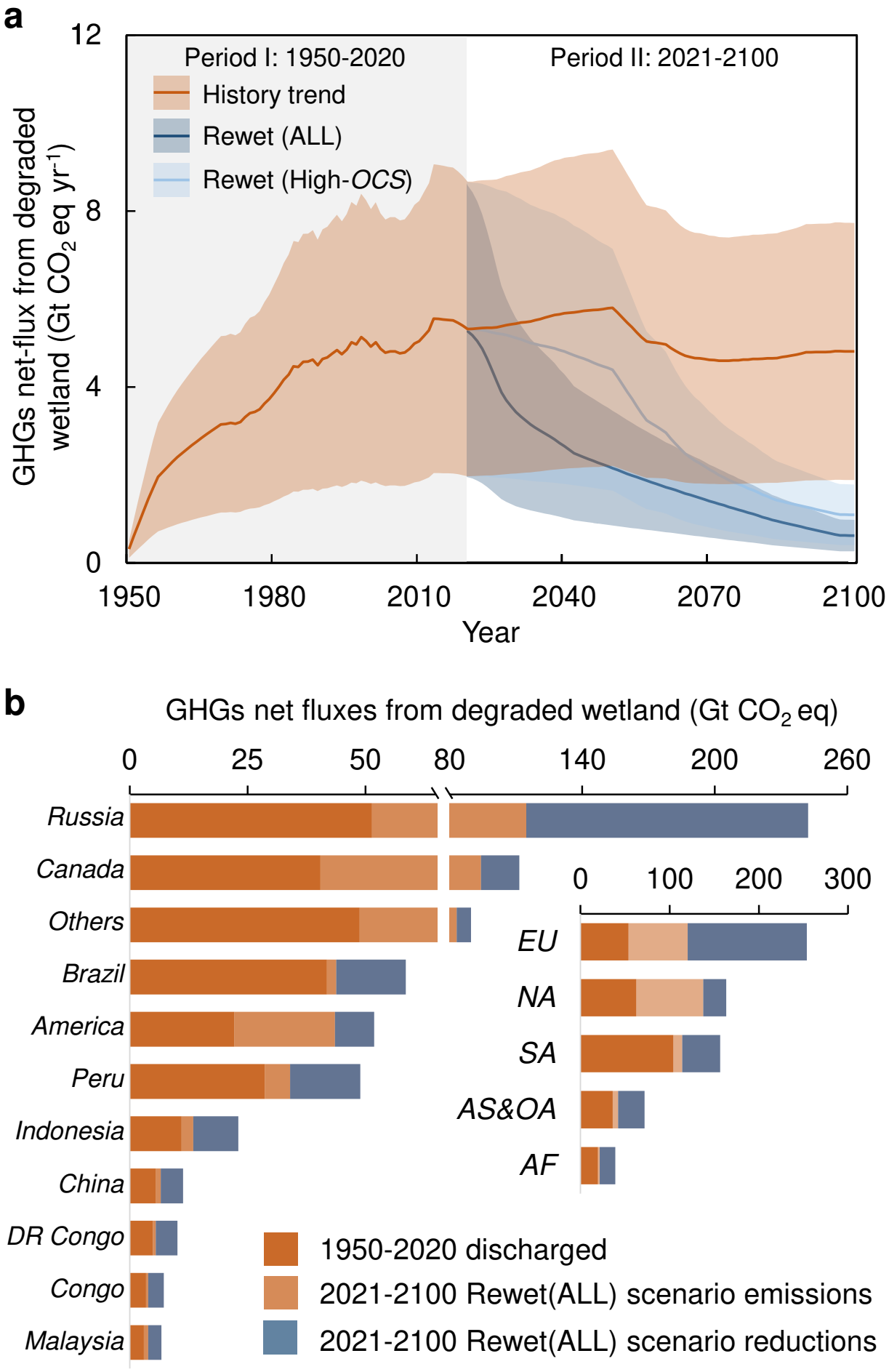
a
Period I: 1950-2020
Period II: 2021-2100
History trend
Rewet (ALL)
Rewet (High-OCS)
GHGs net-flux from degraded wetland (Gt CO2 eq yr-1)
12
8
4
0
1950
1980
2010
2040
2070
2100
Year
b
GHGs net fluxes from degraded wetland (Gt CO2 eq)
0
25
50
80
140
200
260
Russia
Canada
Others
Brazil
America
Peru
Indonesia
China
DR Congo
Congo
Malaysia
0
100
200
300
EU
NA
SA
AS&OA
AF
1950-2020 discharged
2021-2100 Rewet(ALL) scenario emissions
2021-2100 Rewet(ALL) scenario reductions

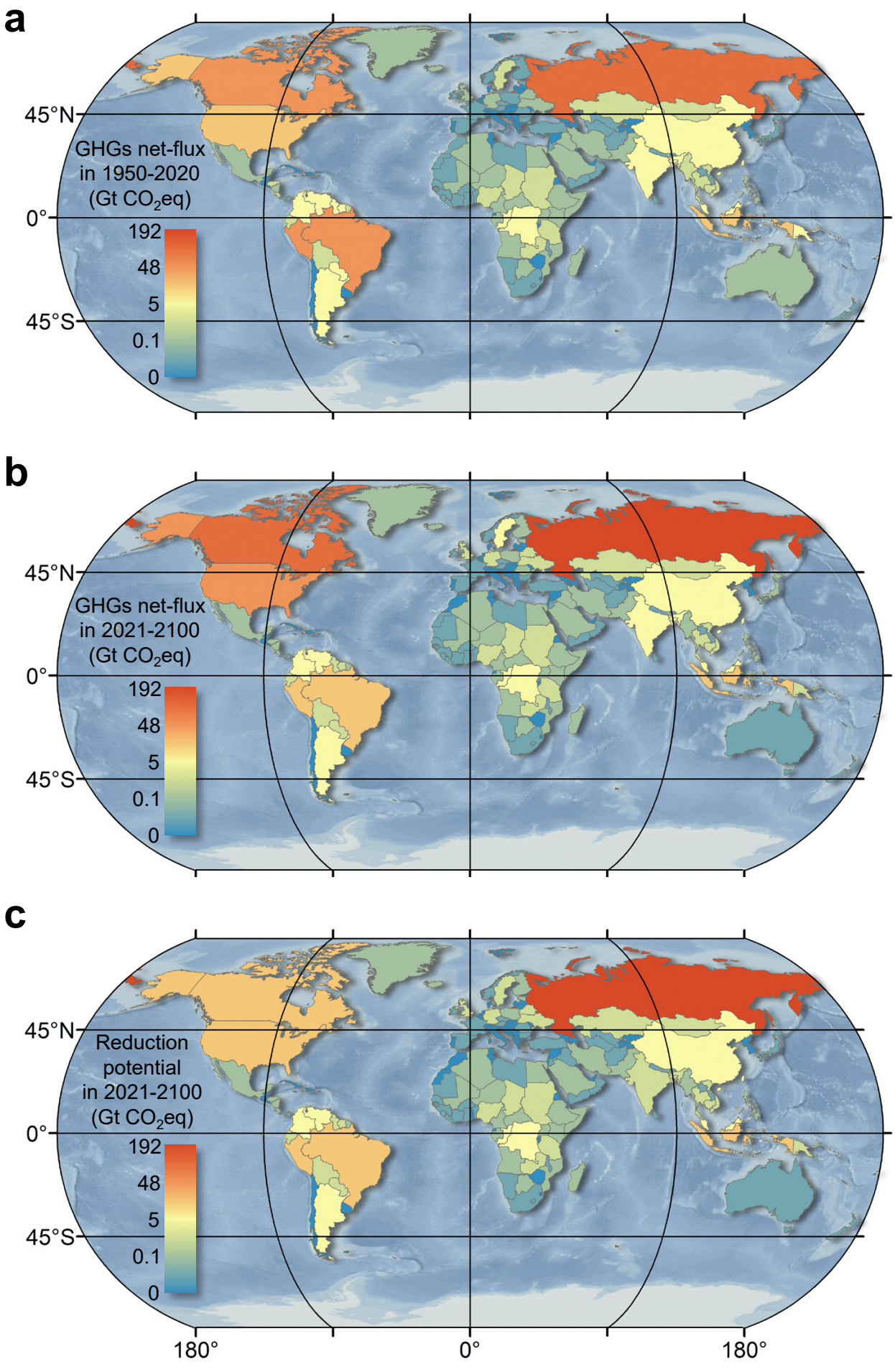
a
45°N
0°
45°S
GHGs net-flux
in 1950-2020
(Gt CO2eq)
192
48
5
0.1
0
b
45°N
0°
45°S
GHGs net-flux
in 2021-2100
(Gt CO2eq)
192
48
5
0.1
0
c
45°N
0°
45°S
Reduction
potential
in 2021-2100
(Gt CO2eq)
192
48
5
0.1
0
180°
0°
180°

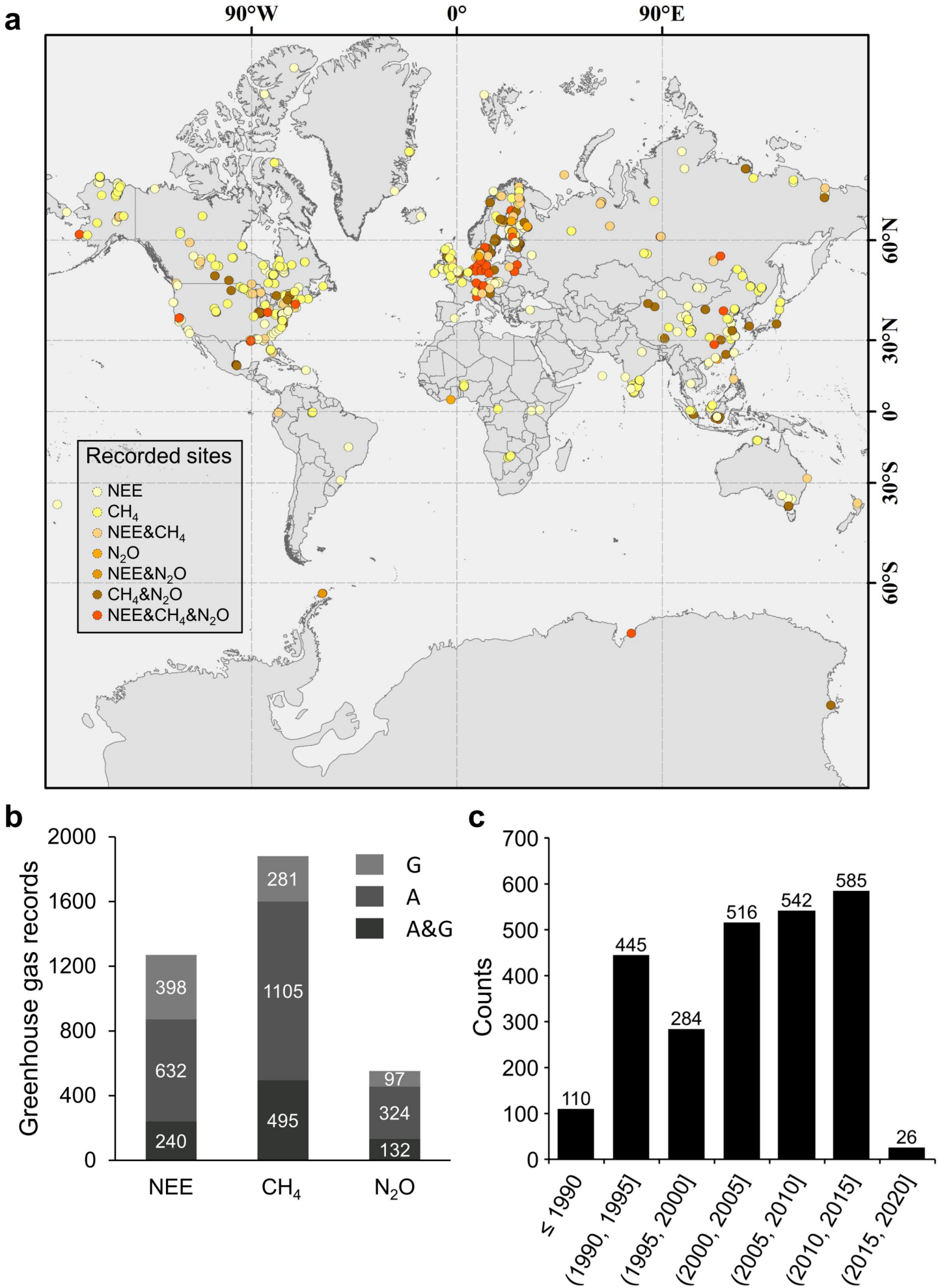
a
90°W
0°
90°E
60°N
30°N
0°
30°S
60°S
Recorded sites
NEE
CH4
NEE&CH4
N2O
NEE&N2O
CH4&N2O
NEE&CH4&N2O
b
Greenhouse gas records
2000
1600
1200
800
400
0
G
A
A&G
398
632
240
281
1105
495
97
324
132
NEE
CH4
N2O
c
Counts
700
600
500
400
300
200
100
0
110
445
284
516
542
585
26
≤ 1990
(1990, 1995]
(1995, 2000]
(2000, 2005]
(2005, 2010]
(2010, 2015]
(2015, 2020]

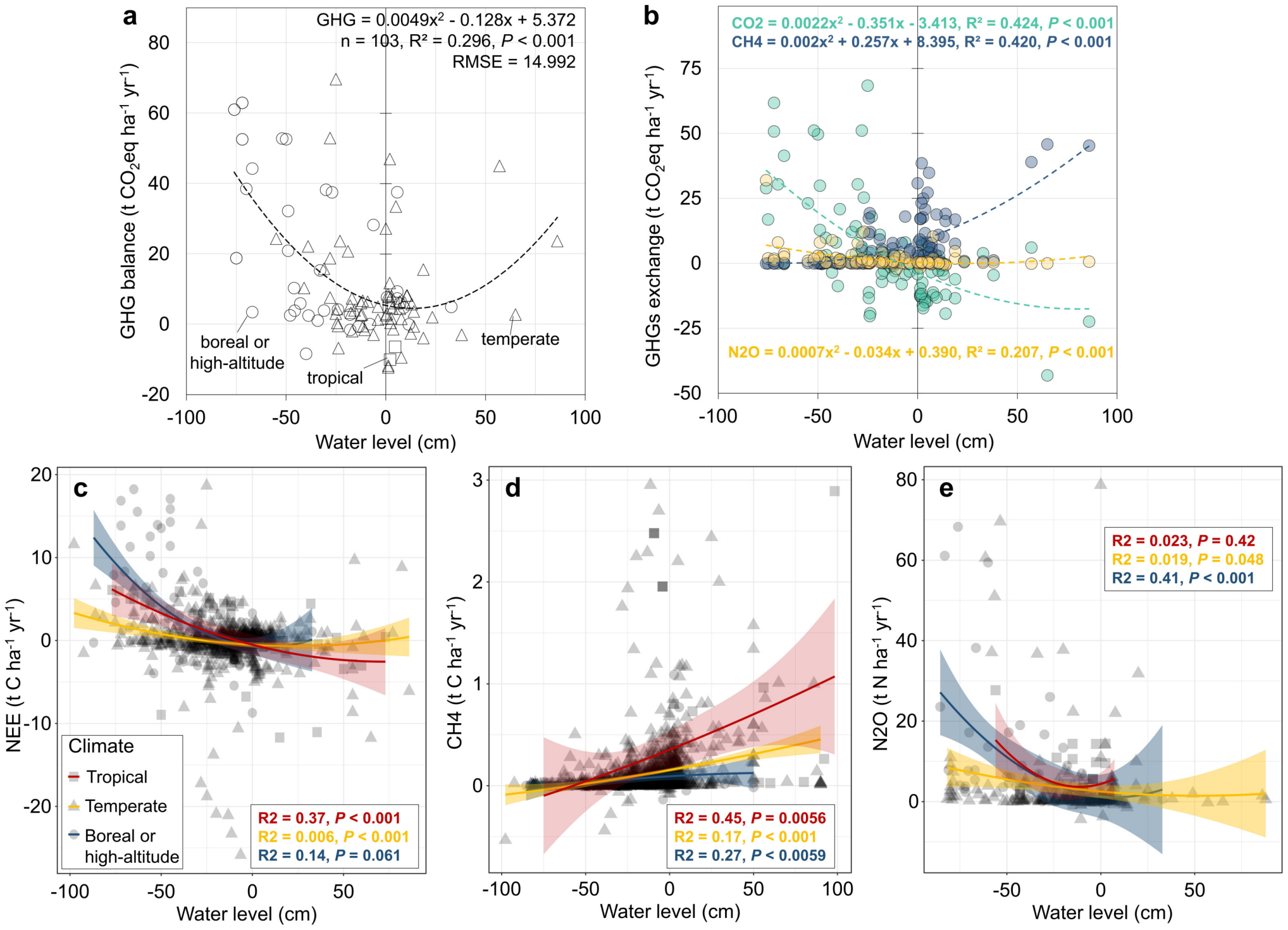
a
GHG = 0.0049x² - 0.128x + 5.372
n = 103, R² = 0.296, P < 0.001
RMSE = 14.992
GHG balance (t CO2eq ha-1 yr-1)
boreal or high-altitude
tropical
temperate
Water level (cm)
b
CO2 = 0.0022x² - 0.351x - 3.413, R² = 0.424, P < 0.001
CH4 = 0.002x² + 0.257x + 8.395, R² = 0.420, P < 0.001
N2O = 0.0007x² - 0.034x + 0.390, R² = 0.207, P < 0.001
GHGs exchange (t CO2eq ha-1 yr-1)
Water level (cm)
c
NEE (t C ha-1 yr-1)
Climate
Tropical
Temperate
Boreal or high-altitude
R2 = 0.37, P < 0.001
R2 = 0.006, P < 0.001
R2 = 0.14, P = 0.061
Water level (cm)
d
CH4 (t C ha-1 yr-1)
R2 = 0.45, P = 0.0056
R2 = 0.17, P < 0.001
R2 = 0.27, P < 0.0059
Water level (cm)
e
N2O (t N ha-1 yr-1)
R2 = 0.023, P = 0.42
R2 = 0.019, P = 0.048
R2 = 0.41, P < 0.001
Water level (cm)

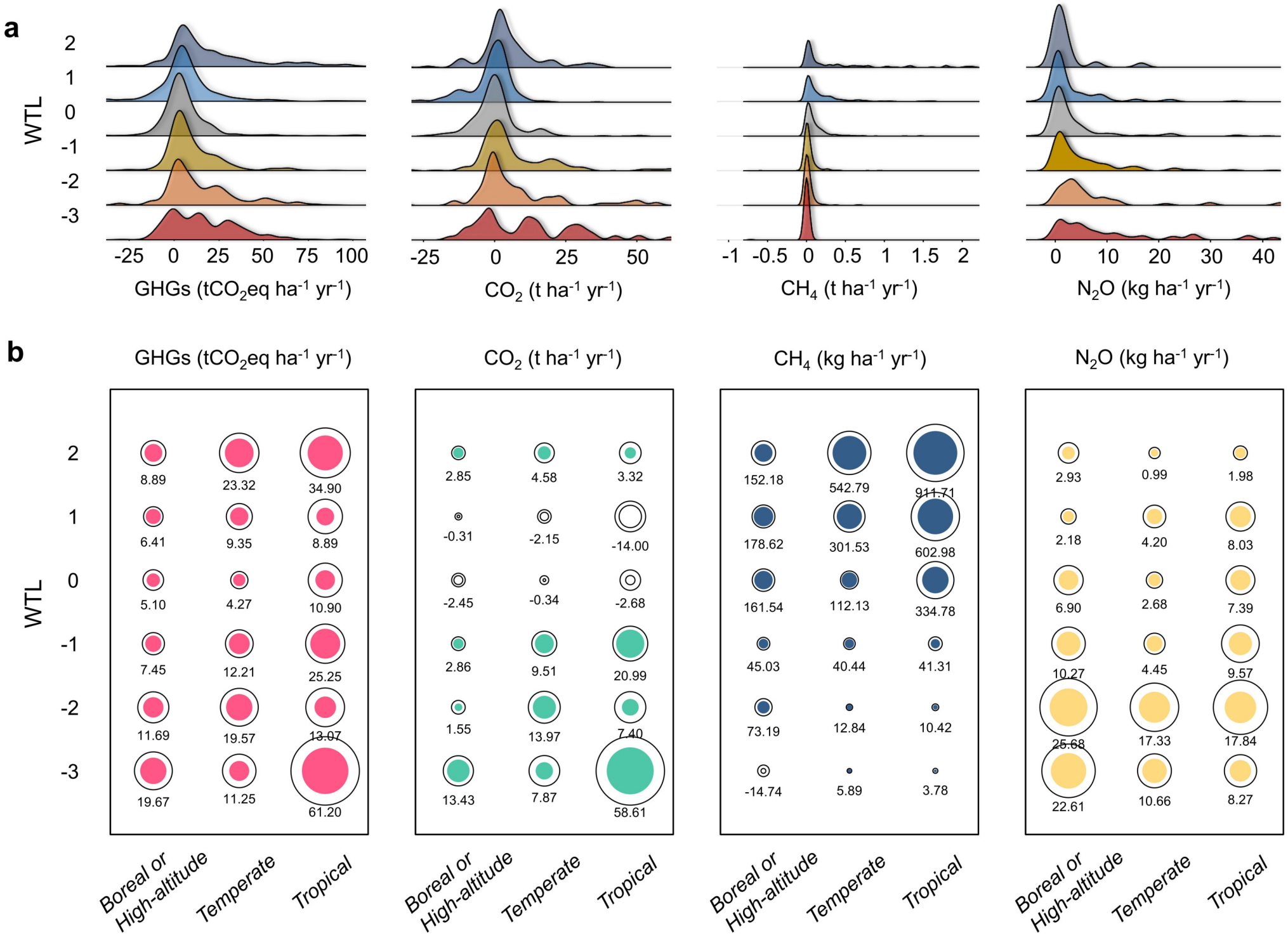
a
WTL
2
1
0
-1
-2
-3
-25 0 25 50 75 100
GHGs (tCO2eq ha-1 yr-1)
-25 0 25 50
CO2 (t ha-1 yr-1)
-1 -0.5 0 0.5 1 1.5 2
CH4 (t ha-1 yr-1)
0 10 20 30 40
N2O (kg ha-1 yr-1)
b
GHGs (tCO2eq ha-1 yr-1)
CO2 (t ha-1 yr-1)
CH4 (kg ha-1 yr-1)
N2O (kg ha-1 yr-1)
WTL
8.89 23.32 34.90
6.41 9.35 8.89
5.10 4.27 10.90
7.45 12.21 25.25
11.69 19.57 13.07
19.67 11.25 61.20
2.85 4.58 3.32
-0.31 -2.15 -14.00
-2.45 -0.34 -2.68
2.86 9.51 20.99
1.55 13.97 7.40
13.43 7.87 58.61
152.18 542.79 911.71
178.62 301.53 602.98
161.54 112.13 334.78
45.03 40.44 41.31
73.19 12.84 10.42
-14.74 5.89 3.78
2.93 0.99 1.98
2.18 4.20 8.03
6.90 2.68 7.39
10.27 4.45 9.57
25.68 17.33 17.84
22.61 10.66 8.27
Boreal or High-altitude
Temperate
Tropical

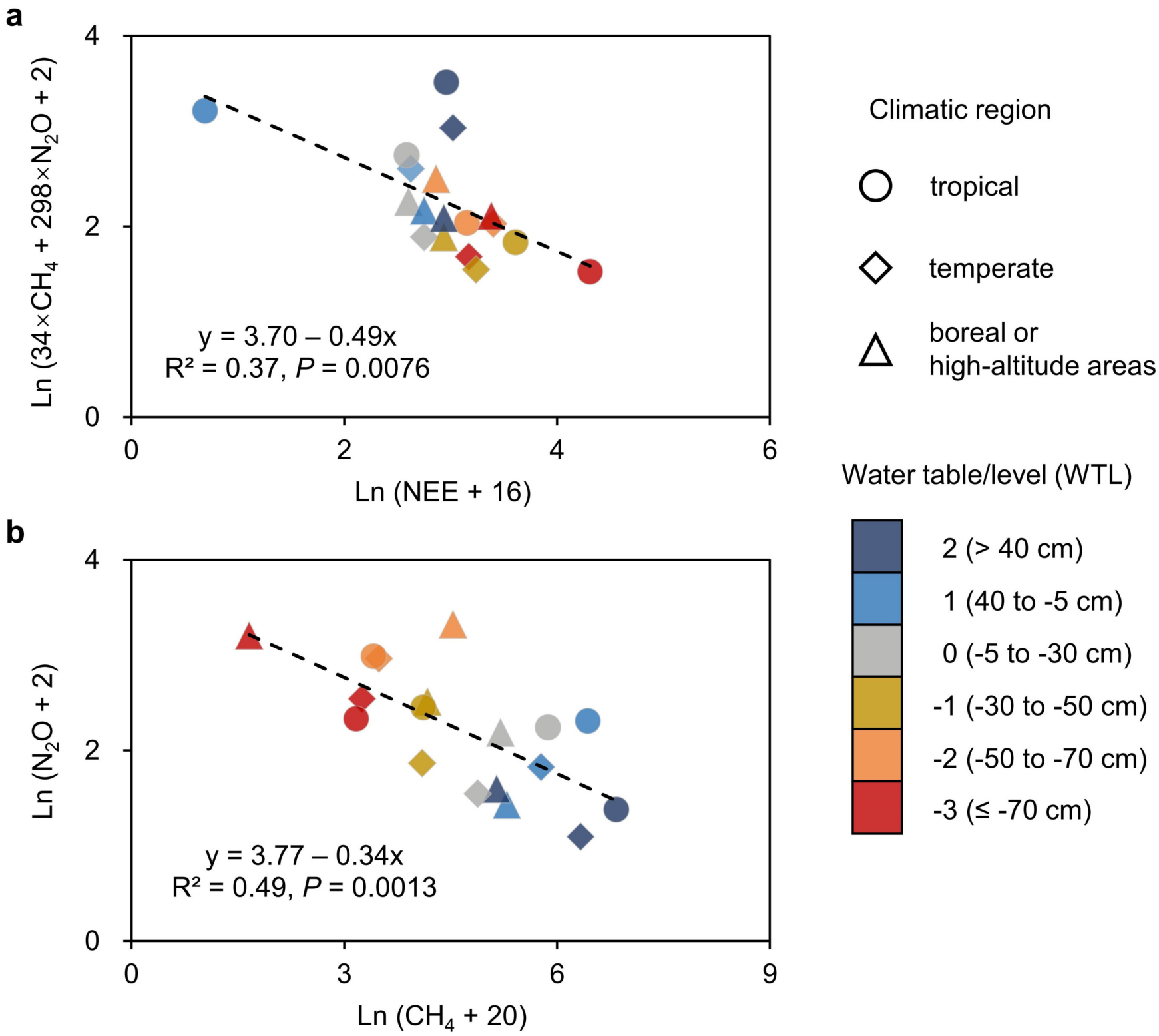
a
Ln (34×CH4 + 298×N2O + 2)
Ln (NEE + 16)
y = 3.70 – 0.49x
R² = 0.37, P = 0.0076
b
Ln (N2O + 2)
Ln (CH4 + 20)
y = 3.77 – 0.34x
R² = 0.49, P = 0.0013
Climatic region
tropical
temperate
boreal or
high-altitude areas
Water table/level (WTL)
2 (> 40 cm)
1 (40 to -5 cm)
0 (-5 to -30 cm)
-1 (-30 to -50 cm)
-2 (-50 to -70 cm)
-3 (≤ -70 cm)

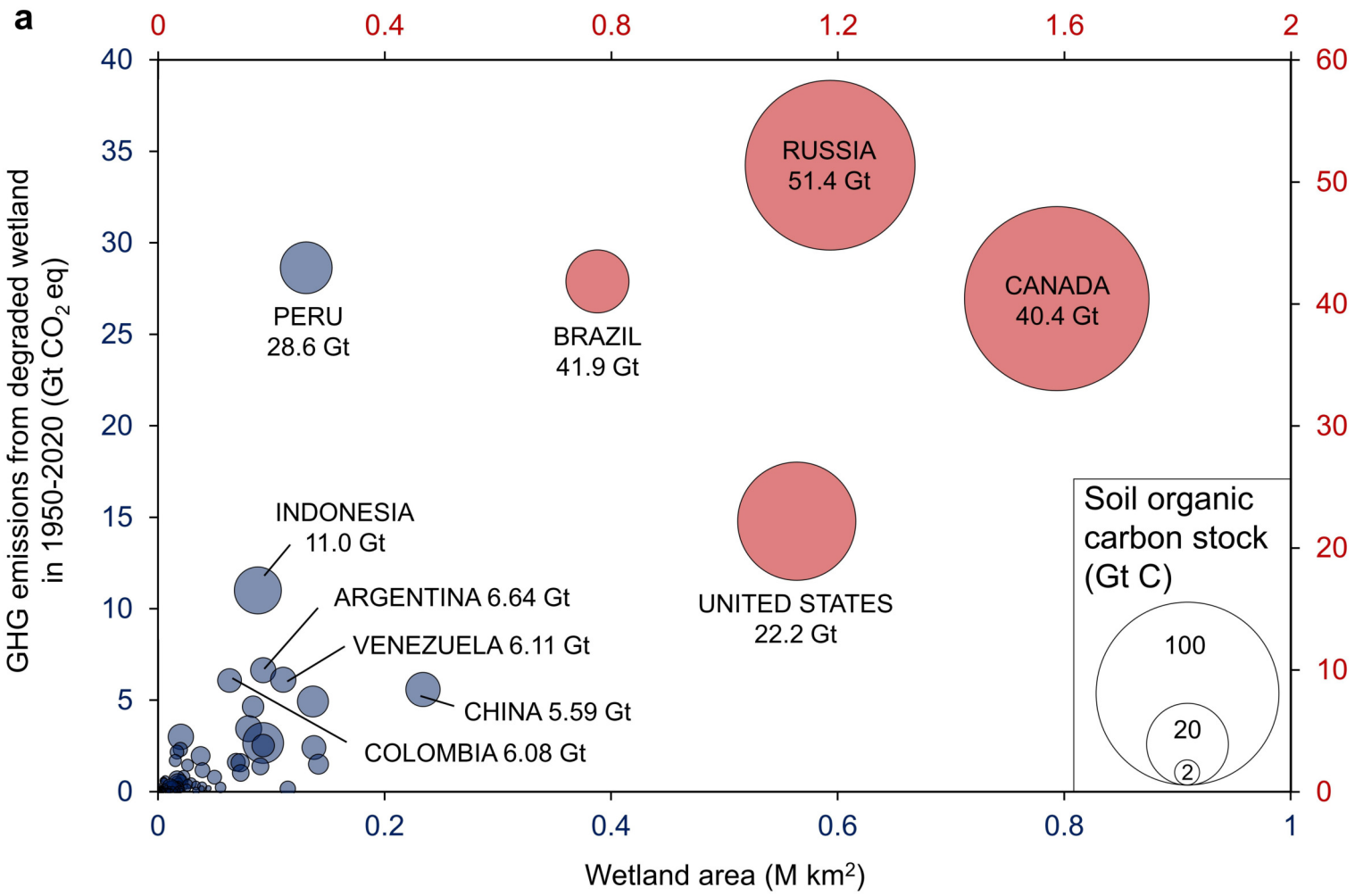
a
GHG emissions from degraded wetland in 1950-2020 (Gt CO_2 eq)
Wetland area (M km^2)
RUSSIA
51.4 Gt
CANADA
40.4 Gt
BRAZIL
41.9 Gt
PERU
28.6 Gt
UNITED STATES
22.2 Gt
INDONESIA
11.0 Gt
ARGENTINA 6.64 Gt
VENEZUELA 6.11 Gt
CHINA 5.59 Gt
COLOMBIA 6.08 Gt
Soil organic carbon stock (Gt C)
100
20
2

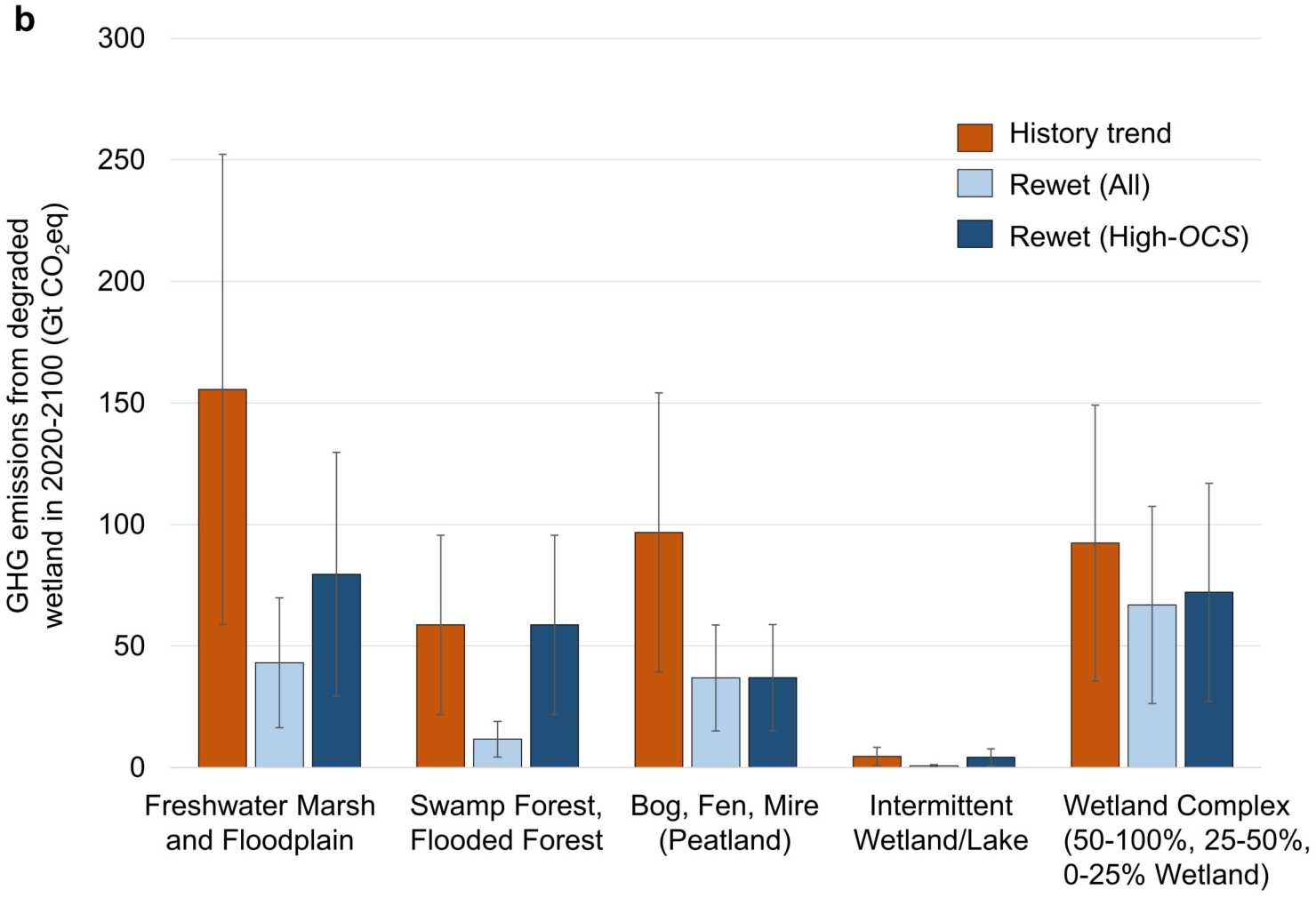
b
GHG emissions from degraded wetland in 2020-2100 (Gt CO_2eq)
History trend
Rewet (All)
Rewet (High-*OCS*)
Freshwater Marsh and Floodplain
Swamp Forest, Flooded Forest
Bog, Fen, Mire (Peatland)
Intermittent Wetland/Lake
Wetland Complex (50-100%, 25-50%, 0-25% Wetland)

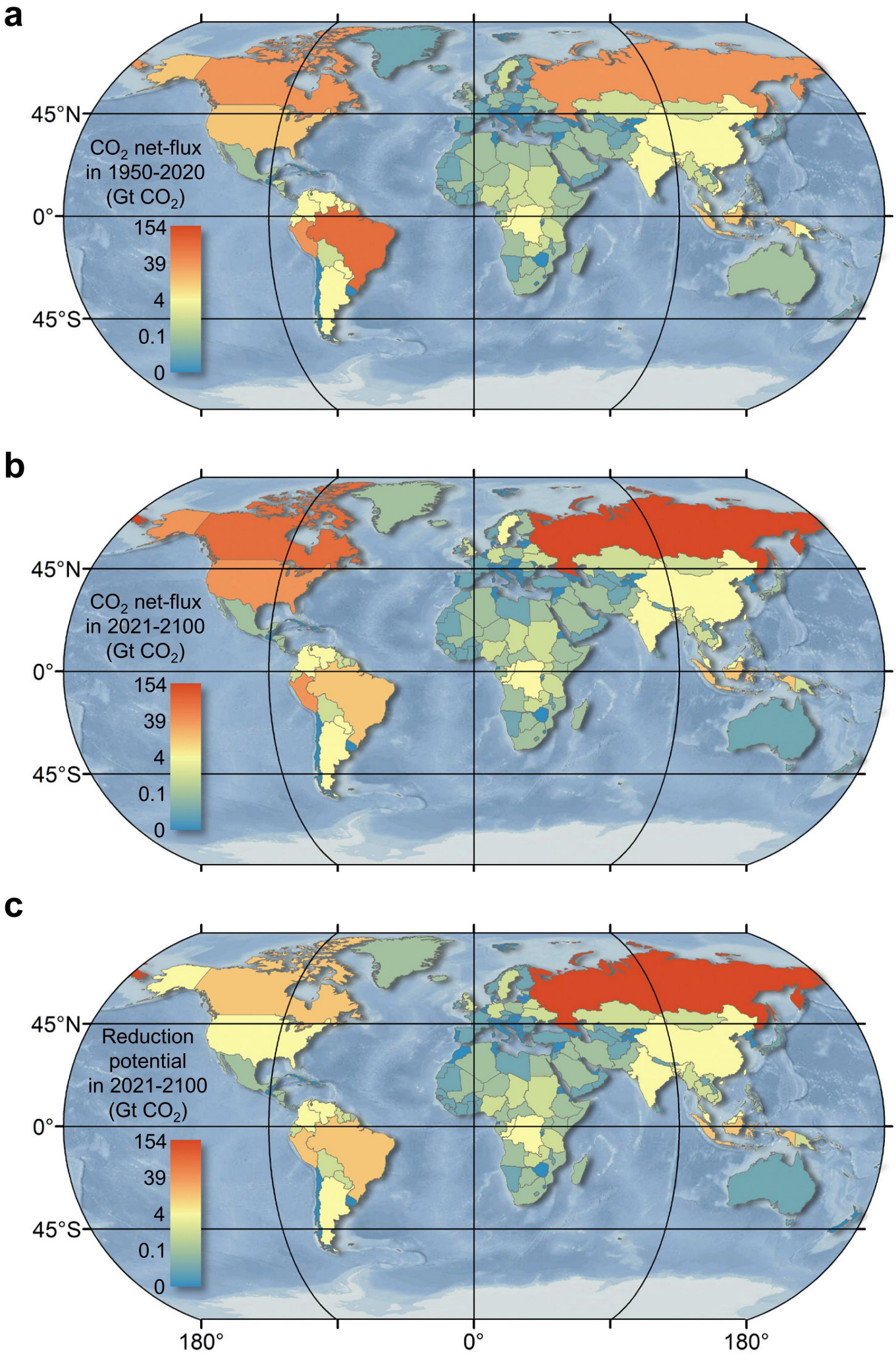
a
45°N
0°
45°S
CO_2 net-flux
in 1950-2020
(Gt CO_2)
154
39
4
0.1
0
b
45°N
0°
45°S
CO_2 net-flux
in 2021-2100
(Gt CO_2)
154
39
4
0.1
0
c
45°N
0°
45°S
Reduction
potential
in 2021-2100
(Gt CO_2)
154
39
4
0.1
0
180°
0°
180°

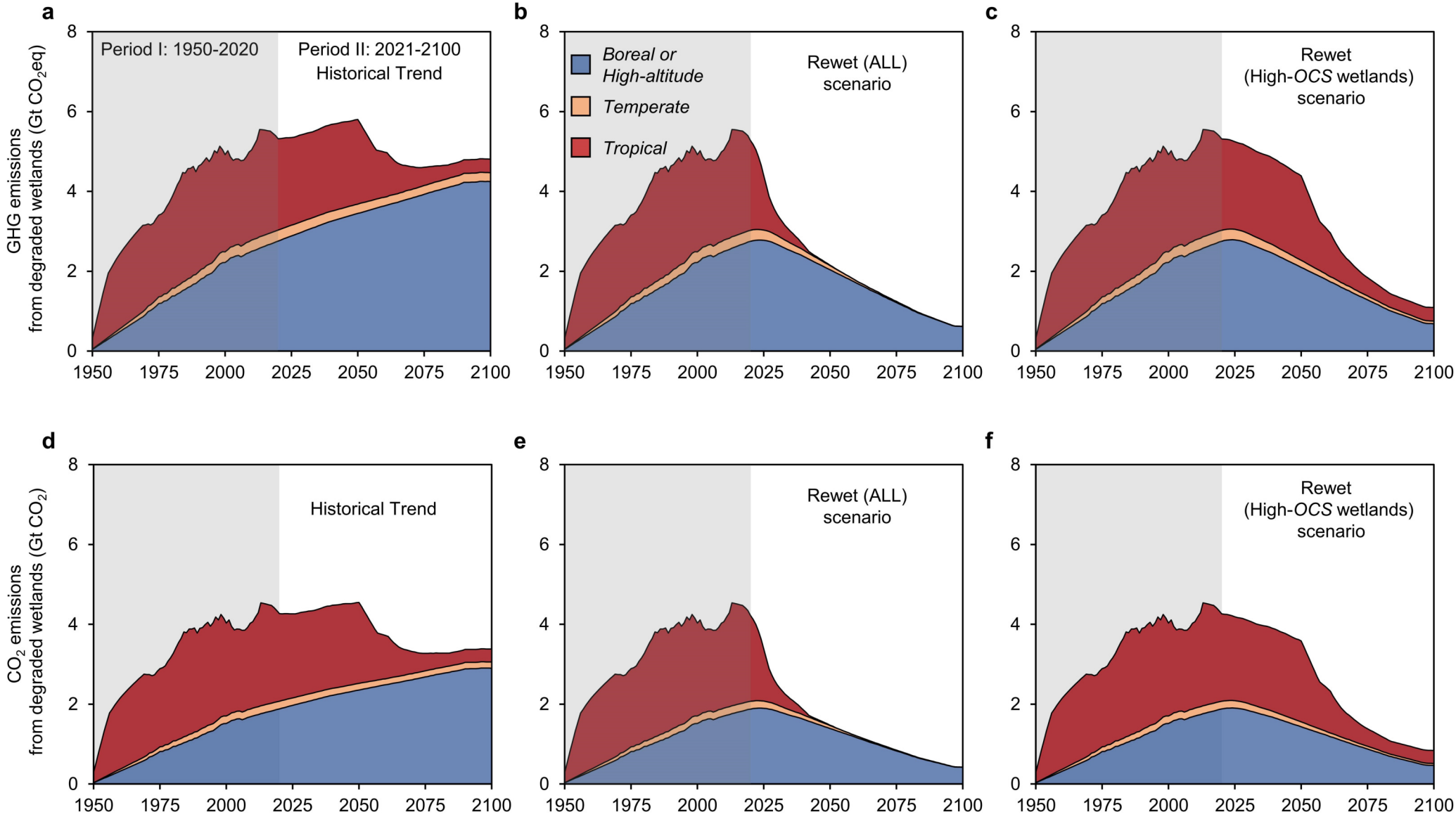
a
b
c
d
e
f
GHG emissions from degraded wetlands (Gt CO_2eq)
CO_2 emissions from degraded wetlands (Gt CO_2)
Period I: 1950-2020
Period II: 2021-2100
Historical Trend
Boreal or High-altitude
Temperate
Tropical
Rewet (ALL) scenario
Rewet (High-OCS wetlands) scenario
0
2
4
6
8
1950
1975
2000
2025
2050
2075
2100

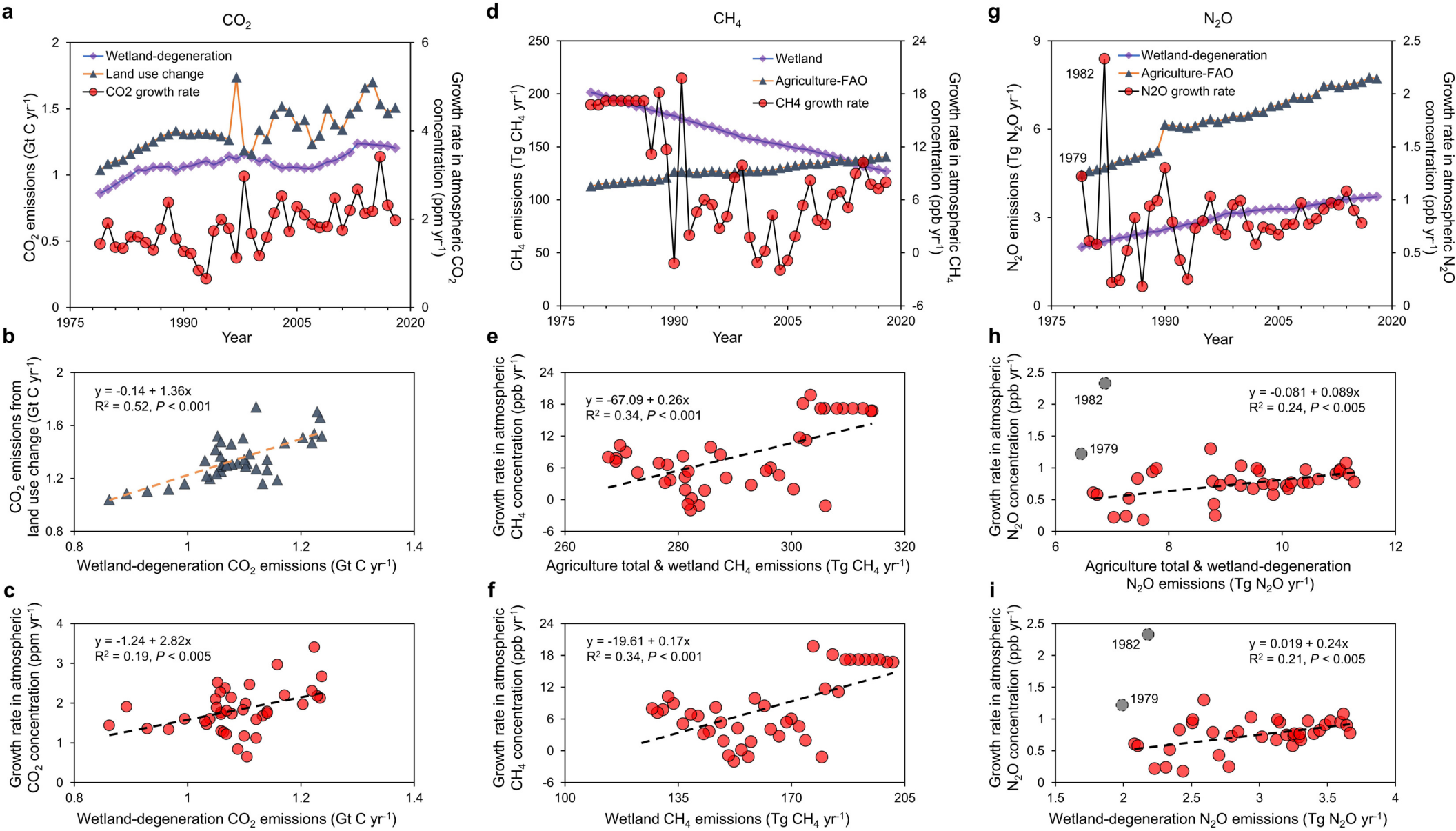
a
CO2
Wetland-degeneration
Land use change
CO2 growth rate
CO2 emissions (Gt C yr-1)
Growth rate in atmospheric CO2 concentration (ppm yr-1)
Year
d
CH4
Wetland
Agriculture-FAO
CH4 growth rate
CH4 emissions (Tg CH4 yr-1)
Growth rate in atmospheric CH4 concentration (ppb yr-1)
Year
g
N2O
Wetland-degeneration
Agriculture-FAO
N2O growth rate
1982
1979
N2O emissions (Tg N2O yr-1)
Growth rate in atmospheric N2O concentration (ppb yr-1)
Year
b
y = -0.14 + 1.36x
R2 = 0.52, P < 0.001
CO2 emissions from land use change (Gt C yr-1)
Wetland-degeneration CO2 emissions (Gt C yr-1)
e
y = -67.09 + 0.26x
R2 = 0.34, P < 0.001
Growth rate in atmospheric CH4 concentration (ppb yr-1)
Agriculture total & wetland CH4 emissions (Tg CH4 yr-1)
h
y = -0.081 + 0.089x
R2 = 0.24, P < 0.005
1982
1979
Growth rate in atmospheric N2O concentration (ppb yr-1)
Agriculture total & wetland-degeneration N2O emissions (Tg N2O yr-1)
c
y = -1.24 + 2.82x
R2 = 0.19, P < 0.005
Growth rate in atmospheric CO2 concentration (ppm yr-1)
Wetland-degeneration CO2 emissions (Gt C yr-1)
f
y = -19.61 + 0.17x
R2 = 0.34, P < 0.001
Growth rate in atmospheric CH4 concentration (ppb yr-1)
Wetland CH4 emissions (Tg CH4 yr-1)
i
y = 0.019 + 0.24x
R2 = 0.21, P < 0.005
1982
1979
Growth rate in atmospheric N2O concentration (ppb yr-1)
Wetland-degeneration N2O emissions (Tg N2O yr-1)

Extended Data Table 1. Wetland greenhouse gas (GHG) net fluxes in different climate regimes under various water level groups (*WTL*).

	Boreal		*Temperate*		*Tropical*	
WTL	**GHGs**	**95%CI**	**GHGs**	**95%CI**	**GHGs**	**95%CI**
2	8.89	4.82	23.32	10.45	34.90	18.78
1	6.41	2.24	9.35	5.56	8.89	16.89
0	5.10	4.36	4.27	2.46	10.90	14.37
-1	7.45	3.48	12.21	4.69	25.25	8.20
-2	11.69	9.38	19.57	11.45	13.07	19.39
-3	19.67	11.34	11.25	13.18	61.20*	38.50*

unit: $tCO_2eq\ ha^{-1}\ yr^{-1}$; * data from J. Leifeld *et al.*, 2019 (ref. 19).

Extended Data Table 2. Wetland characteristics and GHG emissions for each continent per indicated period.

Continent	Area (million km²)	*OCS** (Gt C)	GHG net-flux from degraded wetland (Gt CO_2eq)			
			1950-2020 discharged	2021-2100 projected from historical trend	2021-2100 rewetting all wetlands scenario	2021-2100 rewetting high OCS wetlands scenario
Europe	1.27	99.51	53.94 ± 32.66 (68.38%)†	199.70 ± 120.69 (68.38%)	66.11 ± 39.93 (68.37%)	66.40 ± 40.26 (68.39%)
North America	2.71	158.81	62.64 ± 40.67 (70.19%)	100.77 ± 61.55 (68.69%)	75.05 ± 45.28 (68.41%)	78.25 ± 48.36 (68.79%)
Latin America	1.37	31.05	104.15 ± 65.83 (95.62%)	52.39 ± 33.17 (95.57%)	9.95 ± 6.31 (95.50%)	52.39 ± 33.17 (95.57%)
Asia & Oceania	1.23	26.88	36.07 ± 23.96 (89.83%)	35.70 ± 23.93 (89.03%)	6.17 ± 4.22 (87.34%)	35.08 ± 23.32 (89.38%)
Africa	1.08	13.23	19.64 ± 12.37 (95.73%)	19.30 ± 12.18 (95.67%)	1.87 ± 1.18 (95.52%)	19.30 ± 12.18 (95.67%)
Total	7.66	329.48	276.44 ± 175.49 (83.80%)	407.87 ± 251.51 (75.05%)	159.14 ± 96.92 (71.14%)	251.42 ± 157.28 (79.20%)
Reduction					248.72 ± 154.59 (77.55%)	156.44 ± 94.23 (68.37%)

*: *OCS* represents organic carbon stocks in soil layers from zero to one meter deep. †: The figures in the parentheses indicate the percentage of CO_2 emissions.